JOURNAL OF GEOPHYSICAL RESEARCH, VOL. 108, NO. D3, 8400, doi:10.1029/2001JD000844, 2003

Photochemical production of ozone in the upper troposphere in association with cumulus convection over Indonesia

K. Kita,[1,2] S. Kawakami,[3] Y. Miyazaki,[1] Y. Higashi,[1] Y. Kondo,[1] N. Nishi,[4] M. Koike,[5] D. R. Blake,[6] T. Machida,[7] T. Sano,[3] W. Hu,[8] M. Ko,[8] and T. Ogawa[3]

Received 7 May 2001; revised 5 November 2001; accepted 20 November 2001; published 20 November 2002.

[1] The Biomass Burning and Lightning Experiment phase A (BIBLE-A) aircraft observation campaign was conducted from 24 September to 10 October 1998, during a La Niña period. During this campaign, distributions of ozone and its precursors (NO, CO, and nonmethane hydrocarbons (NMHCs)) were observed over the tropical Pacific Ocean, Indonesia, and northern Australia. Mixing ratios of ozone and its precursors were very low at altitudes between 0 and 13.5 km over the tropical Pacific Ocean. The mixing ratios of ozone precursors above 8 km over Indonesia were often significantly higher than those over the tropical Pacific Ocean, even though the prevailing easterlies carried the air from the tropical Pacific Ocean to over Indonesia within several days. For example, median NO and CO mixing ratios in the upper troposphere were 12 parts per trillion (pptv) and 72 parts per billion (ppbv) over the tropical Pacific Ocean and were 83 pptv and 85 ppbv over western Indonesia, respectively. Meteorological analyses and high ethene (C_2H_4) mixing ratios indicate that the increase of the ozone precursors was caused by active convection over Indonesia through upward transport of polluted air, mixing, and lightning all within the few days prior to observation. Sources of ozone precursors are discussed by comparing correlations of some NMHCs and CH_3Cl concentrations with CO between the lower and upper troposphere. Biomass burning in Indonesia was nearly inactive during BIBLE-A and was not a dominant source of the ozone precursors, but urban pollution and lightning contributed importantly to their increases. The increase in ozone precursors raised net ozone production rates over western Indonesia in the upper troposphere, as shown by a photochemical model calculation. However, the ozone mixing ratio ($\sim$20 ppbv) did not increase significantly over Indonesia because photochemical production of ozone did not have sufficient time since the augmentation of ozone precursors. Backward trajectories show that many air masses sampled over the ocean south of Indonesia and over northern Australia passed over western Indonesia 4–9 days prior to being measured. In these air masses the mixing ratios of ozone precursors, except for short-lived species, were similar to those over western Indonesia. In contrast, the ozone mixing ratio was higher by about 10 ppbv than that over Indonesia, indicating that photochemical production of ozone occurred during transport from Indonesia. The average rate of ozone increase (1.8 ppbv/d) during this transport is similar to the net ozone formation rate calculated by the photochemical model. This study shows that active convection over Indonesia carried polluted air upward from the surface and had a discernable influence on the distribution of ozone in the upper troposphere over the Indian Ocean, northern Australia, and the south subtropical Pacific Ocean, combined with NO production by lightning. *INDEX TERMS:* 0315 Atmospheric Composition and Structure: Biosphere/atmosphere interactions; 0345 Atmospheric Composition and Structure: Pollution—urban and regional (0305); 0368 Atmospheric Composition and Structure: Troposphere—constituent transport and chemistry; *KEYWORDS:* ozone, tropospheric chemistry, biomass burning, convection, vertical transport, aircraft observation

[1]Research Center for Advanced Science and Technology, University of Tokyo, Tokyo, Japan.
[2]Now at Department of Environmental Sciences, Faculty of Science, Ibaraki University, Ibaraki, Japan.
[3]Earth Observing Research Center, National Space Development Agency of Japan, Tokyo, Japan.
[4]Department of Geophysics, Kyoto University, Kyoto, Japan.
[5]Department of Earth and Planetary Science, University of Tokyo, Tokyo, Japan.
[6]Department of Chemistry, University of California, Irvine, California, USA.
[7]National Institute of Environmental Studies, Ibaraki, Japan.
[8]Atmospheric and Environmental Research, Inc., Lexington, Massachusetts, USA.

0148-0227/02/2001JD000844$09.00

Citation: Kita, K., et al., Photochemical production of ozone in the upper troposphere in association with cumulus convection over Indonesia, *J. Geophys. Res.*, *107*, 8400, doi:10.1029/2001JD000844, 2002. [printed *108*(D3), 2003]

1. Introduction

[2] The budget of tropospheric ozone in the tropics is influenced by several processes specific to this region: biomass burning, lightning, strong convection, and transport from midlatitudes. In Southeast Asia, especially in Indonesia, it has been recognized that emissions of ozone precursors, such as nitric oxide (NO), reactive nitrogen (NO_y), carbon monoxide (CO), and nonmethane hydrocarbons (NMHCs) by biomass burning in this region can significantly affect the ozone distribution. Ozonesonde observations have revealed the seasonal variation of tropospheric ozone over Indonesia, indicating that the ozone mixing ratio in the lower and middle troposphere increases in the late dry season (August to November), probably due to biomass burning [*Komala et al.*, 1996; *Fujiwara et al.*, 2000]. The observations also showed that the remarkably large ozone increase persisted between September and November in 1994 and 1997 when extensive forest fires occurred in Indonesia [*Fujiwara et al.*, 1999]. Airborne observations [*Matsueda and Inoue*, 1999; *Sawa et al.*, 1999; *Tsutsumi et al.*, 1999] and satellite remote sensing data [*Connors et al.*, 1999; *Burrows et al.*, 1999] in the same times indicated that the amounts of ozone precursors increased significantly around Indonesia. Satellite total ozone data showed that the increases in tropospheric ozone spread over Indonesia and the nearby Indian Ocean in these times and that similar ozone increases often appeared during other El Niño periods [*Chandra et al.*, 1998; *Ziemke and Chandra*, 1999; *Thompson and Hudson*, 1999; *Kita et al.*, 2000]. While the influence from other processes such as long-range transport, convection, and lightning [*Chandra et al.*, 1998; *Hauglustein et al.*, 1999; *Kita et al.*, 2000; *Thompson et al.*, 2001] can also contribute to the ozone increase, biomass burning clearly plays an important role during El Niño periods.

[3] In contrast, the influence of active convection over Indonesia on the ozone budget during La Niña periods, or wet seasons, is not fully understood. Active convection in the tropics can influence tropospheric ozone through effective upward transport of clean, ozone-poor air from the marine boundary layer [e.g., *Kley et al.*, 1996; *Kawakami et al.*, 1997] or pollutants emitted from surface sources [e.g., *Pickering et al.*, 1991, 1996; *Folkins et al.*, 1997; *Andreae et al.*, 2001] to the free troposphere. In addition, active convection may affect the amount of NO in the upper troposphere through its production by lightning discharge. Comprehensive observations of ozone and its precursors are necessary in order to understand the role of convection over Indonesia on the ozone budget.

[4] The Biomass Burning and Lightning Experiment (BIBLE) campaigns were designed to investigate the ozone budget and the processes that affect it over Indonesia and northern Australia. BIBLE-A, which was carried out in the transition period from dry season to wet season in this region during La Niña in 1998, provided a particularly good opportunity to investigate the influence of active convection over the Indonesian maritime-continent region on the ozone budget, because cumulus convection was more active during BIBLE-A than in other years. In this paper, distributions of ozone and its precursors observed during BIBLE-A over Indonesia and northern Australia are presented together with discussions of their sources and the influence of active convection over Indonesia.

2. Experiment

[5] The data used in this paper were obtained during BIBLE-A, which was conducted between 24 September and 10 October 1998 [*Kondo et al.*, 2002]. This campaign was comprised of one test flight and 14 science flights made by the Gulfstream-II (G-II) research aircraft, which flew from Nagoya, Japan (36°N) to Bandung, Indonesia (7°S) via Saipan (15°N), Biak, Indonesia (1°S), and Darwin, Australia (12°S). The observational flights covered altitudes between 0.2 and 13.5 km. The tropopause height was about 16 km over Indonesia and northern Australia during BIBLE-A.

[6] The BIBLE-A campaign was carried out in the transition from dry to wet season during a La Niña period, when convection and precipitation were active in Indonesia [*Kondo et al.*, 2002; *Nishi*, 2001]. Biomass burning in Indonesia was nearly inactive as compared to other years. The accumulated number of nighttime hot spots (pixels indicating high temperature), which was obtained from the World Fire Atlas provided by European Space Agency (available at http://shark1.esrin.esa.it/ionia/FIRE/AF/ATSR/) using Along Track Scanning Radiometer (ATSR)-2 data, in Sumatra, Borneo, and Java Islands from August to October was about 100 in 1998, while it was about 13,000 in 1997 when extensive forest fires occurred in these islands.

[7] We used the observed data of ozone, NO, NO_y, CO, methyl chloride (CH_3Cl), methyl bromide (CH_3Br), and some selected NMHCs in the present analyses. Water vapor data and photolysis rates derived from the omnidirectional ultraviolet (UV) flux data were also used in the model calculation of ozone formation/destruction rates. The ozone mixing ratio was measured with a dual-beam UV-absorption ozone photometer. The CO mixing ratio was measured onboard the G-II aircraft by using an automated gas chromatograph (GC) system with a reduction gas detector (RGD). NO and NO_y were measured by a chemiluminescence technique [*Kondo et al.*, 1997] with 1-second time resolution. Interference from HCN, CH_3CN, or NH_3 was negligible for the NO_y measurement [*Koike et al.*, 2000]. Methane (CH_4), NMHCs including ethane (C_2H_6), ethene (C_2H_4), ethyne (C_2H_2), propane (C_3H_8), *n*-butane (n-C_4H_{10}), *i*-butane (i-C_4H_{10}), and benzene (C_6H_6), and halocarbons, such as CH_3Cl, were measured by whole air sampling followed by gas chromatographic analysis in the laboratory [*Blake et al.*, 1996a; *Shirai et al.*, 2002]. The air samples were obtained at intervals of 5 minutes on average, with more frequent sampling during ascent or descent of the aircraft. The water vapor concentration was measured by using a CR-2 dew-point hygrometer (Buck Research Instruments, Boulder, USA). Omnidirectional UV flux was measured to evaluate the photolysis rate coefficients, $J(NO_2)$ for NO_2 photolysis and $J(O^1D)$ for $O_3 + h\upsilon \rightarrow O(^1D) + O_2$, by using filter radiometers (Meteorologie Consult, Koenigstein,

Germany) [*Junkermann et al.*, 1989; *Volz-Thomas et al.*, 1996; *Crawford et al.*, 1999]. More detailed descriptions of the measurements of ozone, CO, and UV flux are given in the Appendix A. The observed data were averaged over a common interval of 60 s for the present analysis. For the correlation with NMHCs, the other data were averaged over the sampling time of the NMHCs measurements.

3. Results and Discussion

3.1. Distribution of Ozone and Its Precursors Over Indonesia

[8] Figure 1 shows the horizontal distribution of ozone, NO, NO_y, CO, C_2H_6, and C_2H_4 along the G-II flight tracks in the upper troposphere between 8 and 13.5 km during BIBLE-A. While mixing ratios of all these species were low over the tropical Pacific Ocean (defined by the region covering 16°N–2.5°S and 135°E–150°E), simultaneous increases in the mixing ratios of CO, NO, NO_y, C_2H_6, and C_2H_4 were frequently observed in the upper troposphere over eastern (7°N–9°S, 108°E–135°E) and western Indonesia (7°N–9°S, 95°E–108°E). Several other NMHCs including C_2H_2, C_3H_8, *n*-C_4H_{10}, *i*-C_4H_{10}, and C_6H_6 also increased over these regions (not shown). The median mixing ratios of ozone, NO, NO_y, CO, C_2H_6, C_2H_4, C_2H_2, and C_3H_8 in the upper troposphere over the above three regions are compared in Figure 2 and are listed in Table 1. The median values in the Indonesian outflow air and the midlatitude/African air, described below, are also given. The median mixing ratios of all species increased from east (tropical Pacific Ocean) to west (western Indonesia), north of 9°S. For example, the median mixing ratios of CO and NO_y increased from 72 ppbv and 31 pptv over the tropical Pacific Ocean to 77 ppbv and 75 pptv over eastern Indonesia and 85 ppbv and 221 pptv over western Indonesia, respectively. In western Indonesia, the variability in CO, NO, NO_y, and NMHCs was also larger than that in the other regions. It should be noted that the mixing ratios of short-lived NMHCs such as C_2H_4 also increased (the C_2H_4 mixing ratio often exceeded 50 pptv and its median value was 24.5 pptv) over western Indonesia. C_2H_4 is considered a good indicator of recent influence of surface emissions because its lifetime is relatively short, a few days. The high C_2H_4 mixing ratio indicates that ozone precursors emitted from surface sources, probably in Indonesia, were injected into the observed air masses in the upper troposphere within a few days prior to observation. In contrast to the ozone precursors, the ozone mixing ratios over eastern and western Indonesia were low, similar to that over the tropical Pacific Ocean. As discussed in section 3.4, ozone photochemical production had not proceeded significantly over these regions due to the short elapsed time after the increase of ozone precursor concentrations.

[9] Figure 3 shows altitude profiles of ozone, CO, NO, NO_y, C_2H_6, C_2H_2, and C_3H_8 mixing ratios in the tropical Pacific Ocean, eastern Indonesia, and western Indonesia. The median values and the central 50% of the ranges of the observed mixing ratios for each 1 km in altitude are presented. The median mixing ratios of these species over the tropical Pacific Ocean were low and nearly constant between 0 and 13.5 km (except for 10–11 km). The ozone mixing ratios over eastern and western Indonesia were also nearly constant (15–25 ppbv) in the free troposphere above 3 km. These low and constant ozone mixing ratios in the free troposphere were less than those observed in the September–October period of other years when biomass burning occurred in Indonesia, but were similar to those in the wet season (December–March) [*Komala et al.*, 1996; *Fujiwara et al.*, 2000], consistent with the small biomass burning activity during BIBLE-A. On the contrary, the CO, NO_y, C_2H_6, C_2H_2, and C_3H_8 mixing ratios increased with altitude above 8 km over eastern and western Indonesia. In the lower troposphere below 3 km, the CO mixing ratio often exceeded 80 ppbv in eastern and western Indonesia, and the variability of the CO, NO_y, C_2H_6, C_2H_2, and C_3H_8 mixing ratios was large there, suggesting recent influence by surface sources. These mixing ratios in western Indonesia were similar to or lower than those in eastern Indonesia in this altitude region, suggesting the influence of clean marine air transported from the Indian Ocean by westerly winds over Sumatra Island.

[10] To investigate the origins and transport routes of the observed air masses, 10-day kinematic backward trajectories were calculated for each air mass encountered during the aircraft flights. In the calculation, the European Centre for Medium-Range Weather Forecasts (ECMWF) 2.5° × 2.5° gridded data and a computing program developed by NASDA/EORC [*Matsuzono et al.*, 1998] were used. The vertical displacement of air masses is calculated using the vertical wind component of the ECMWF data. Figure 4a shows the observation points in the upper troposphere over the tropical Pacific Ocean and eastern and western Indonesia together with representative examples of the backward trajectories from eastern and western Indonesia. The trajectories show that upper tropospheric air over western and eastern Indonesia were carried from regions over the tropical Pacific Ocean by the easterlies prevailing over these three regions during BIBLE-A. Median mixing ratios of all the species displayed in Figure 2 increased along this general transport direction over these regions (i.e., tropical Pacific Ocean < eastern Indonesia < western Indonesia), indicating that the increase of ozone precursor concentrations occurred in clean air from the tropical Pacific Ocean during the transport over Indonesia. We will show in sections 3.2 and 3.3 that this increase was caused by the injection of additional ozone precursors into the upper troposphere in association with active convection over Indonesia during BIBLE-A. In general, each backward trajectory is considerably uncertain at active convection areas, because mesoscale wind disturbances and mixing of air masses due to convection is not expressed by the trajectory calculation using the ECMWF data. The trajectories in Figure 4a should be considered to show the average transport pattern during BIBLE-A.

[11] Figure 4b shows representative examples of the backward trajectories calculated for the upper tropospheric air masses observed south of 9°S. These air masses were divided into two groups according to the backward trajectories: Indonesian outflow air and midlatitude/African air. The Indonesian outflow air masses left Indonesia for the Indian Ocean 4 to 9 days prior to the observation and turned to the east over the Indian Ocean south of 15°S due to the prevailing westerlies in this region. Ozone increases in these air masses are discussed in section 3.4. The midlatitude/African air masses traveled eastward south of 20°S, passing

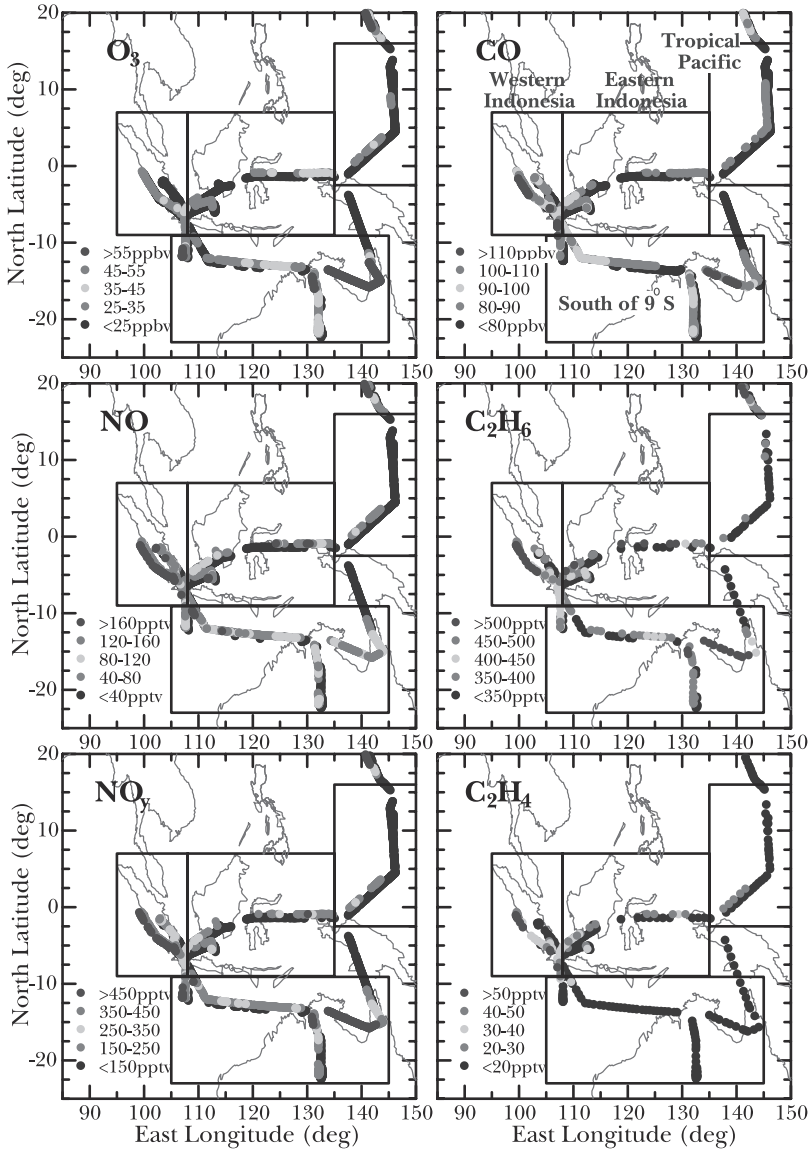

Figure 1. Distribution of ozone, NO, NO_y, CO, C_2H_6, and C_2H_4 in the upper troposphere (8–13.5 km) observed during BIBLE-A. See color version of this figure at back of this issue.

over Africa, and then turned northward prior to the observation. Their chemical characteristics are described by *Kondo et al.* [2002] in detail.

3.2. Convection Over Indonesia

[12] The presence of deep convection over Indonesia was identified by the formation of cumulus clouds reaching the upper troposphere. Upper tropospheric clouds were detected using the infrared (IR) cloud image data obtained by the Geostationary Meteorological Satellite (GMS)-5. The spatial and temporal resolutions of the GMS-5 data used in the present analysis are $0.25° \times 0.25°$ and 1 hour, respectively. Upper tropospheric clouds above 8 km were discriminated by the criterion that their blackbody temperatures (Tbb) evaluated from IR image data were less than 255 K, which corresponds to the average air temperature measured at the 8-km altitude level over Indonesia during BIBLE-A. The influence of optically thin clouds, such as cirrus, was excluded by adopting the criterion that the difference of Tbb evaluated from the two IR channels of GMS-5 (IR channel 1: wavelength 10.5–11.5 μm; and IR channel 2: 11.5–12.5 μm) was less than 0.5 K. The Tbb difference mostly exceeds 1 K in cirrus [*Inoue*, 1985, 1989]. Figure 5a shows the distribution of the upper tropospheric cloud occurrence, which is defined by the percentage of the time when pixels indicating upper tropospheric clouds appeared in each $1° \times 1°$ area in the total observation time period between 24 September and 10 October in 1998, during BIBLE-A. The occurrence of optically thick (probably cumulus) clouds often exceeded 50% in the upper troposphere over Indonesia during this period. A similar distribution for the same period in 1997 is also shown in Figure 5b for comparison, indicating that upper tropospheric clouds occurred much more frequently in 1998, in the transition from dry to wet season during a La Niña period, than in 1997, in the late dry season during an El Niño period.

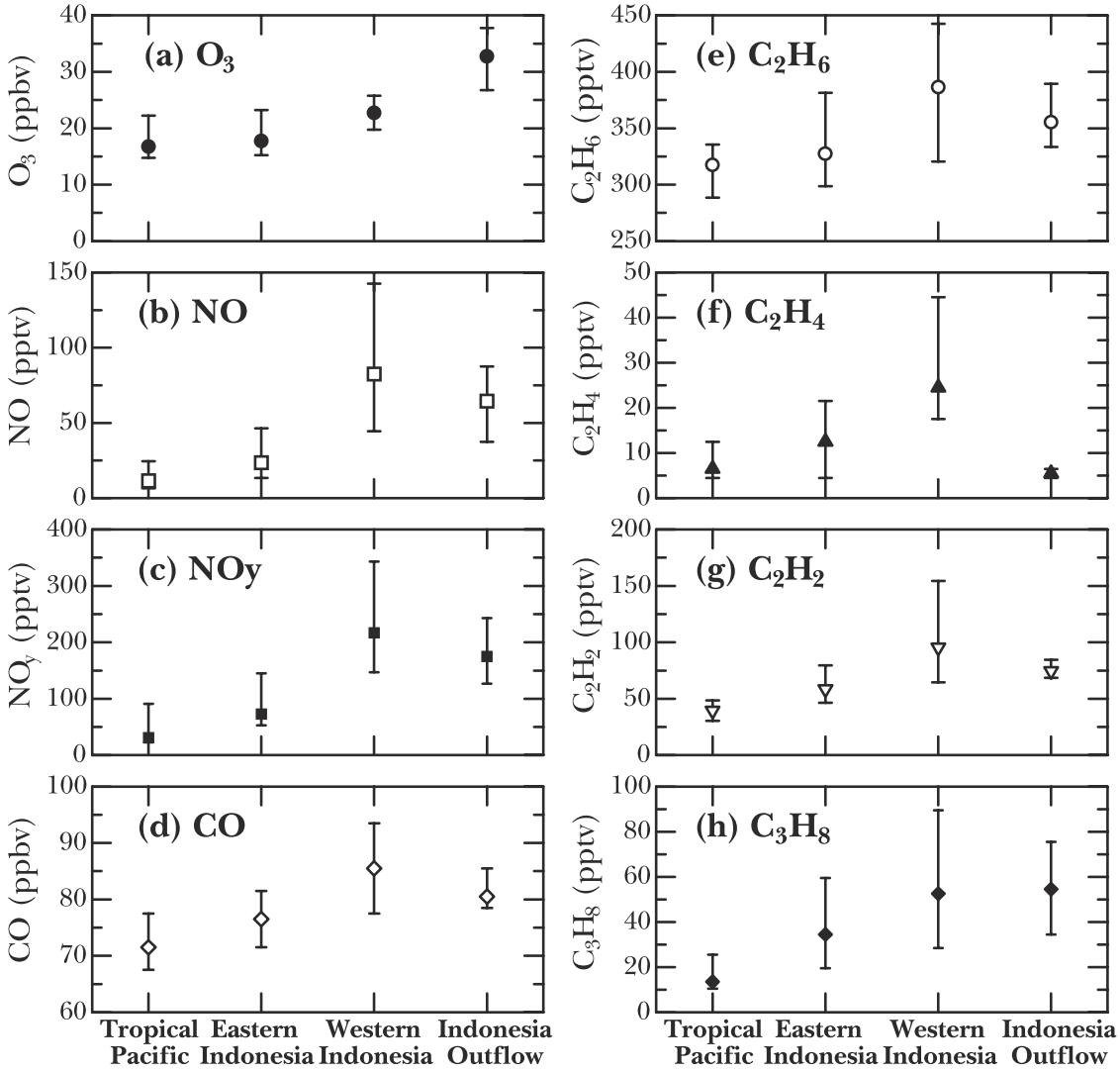

Figure 2. Median mixing ratios of (a) O_3, (b) NO, (c) NO_y, (d) CO, (e) C_2H_6, (f) C_2H_4, (g) C_2H_2, and (h) C_3H_8 in the upper troposphere over the tropical Pacific Ocean, eastern Indonesia, and western Indonesia. Those in the Indonesia outflow air are also shown. Bars indicate the central 50% of the range.

[13] The air masses were likely influenced by convection over Indonesia through the mixing of upper tropospheric air with air lifted from the lower troposphere and through NO production by lightning, if they had encountered cumulus clouds prior to the aircraft observations. Encounters with optically thick (cumulus) clouds were determined by the criterion that Tbb at a point along the backward trajectory for each air mass was lower than the air temperature derived from the ECMWF data at that point. Although the Tbb and air temperature values have some errors, the errors are

Table 1. Median Mixing Ratios of Ozone, NO, NO_y, CO, C_2H_6, C_2H_4, C_2H_2, and CH_3Cl Observed in the Tropical Pacific Ocean, Eastern Indonesia, and Western Indonesia With the Central 50% of the Range[a]

Species	Tropical Pacific Ocean	Eastern Indonesia	Western Indonesia	Indonesian Outflow Air	Midlatitude/ African Air
O_3 (ppbv)	16.8 −1.5/+5.5	18.3 −2.5/+5.5	22.2 −2.5/+3.5	33.2 −6.5/+4.0	75.3 −39.5/+25.5
NO	11 −3/+13	24 −9/+22	77 −36/+57	65 −29/+23	79 −19/+42
NO_y	31 −8/+58	79 −24/+76	221 −76/+104	171 −48/+74	465 −258/+208
CO(ppbv)	71.5 −4.0/+6.0	76.5 −5.0/+4.0	84.5 −7.0/+9.0	80.5 −2/+5.0	90.5 −13.0/+15.0
C_2H_6	318 −29/+18	328 −29/+54	387 −66/+56	356 −22/+34	398 −27/+155
C_2H_4	7 −2/+6	13 −8/+9	25 −7/+20	6 −1/+1	5 −1/+1
C_2H_2	40 −9/+9	59 −12/+21	96 −31/+59	75 −6/+6	80 −18/+33
C_3H_8	14 −3/+12	35 −15/+25	53 −24/+37	55 −20/+21	38 −6/+10
CH_3Cl	549 −15/+10	580 −14/+19	577 −22/+19	570 −12/+5	560 −7/+7

[a] Those in the Indonesian outflow air and the midlatitude/African air are also shown. The units are pptv except for ozone and CO.

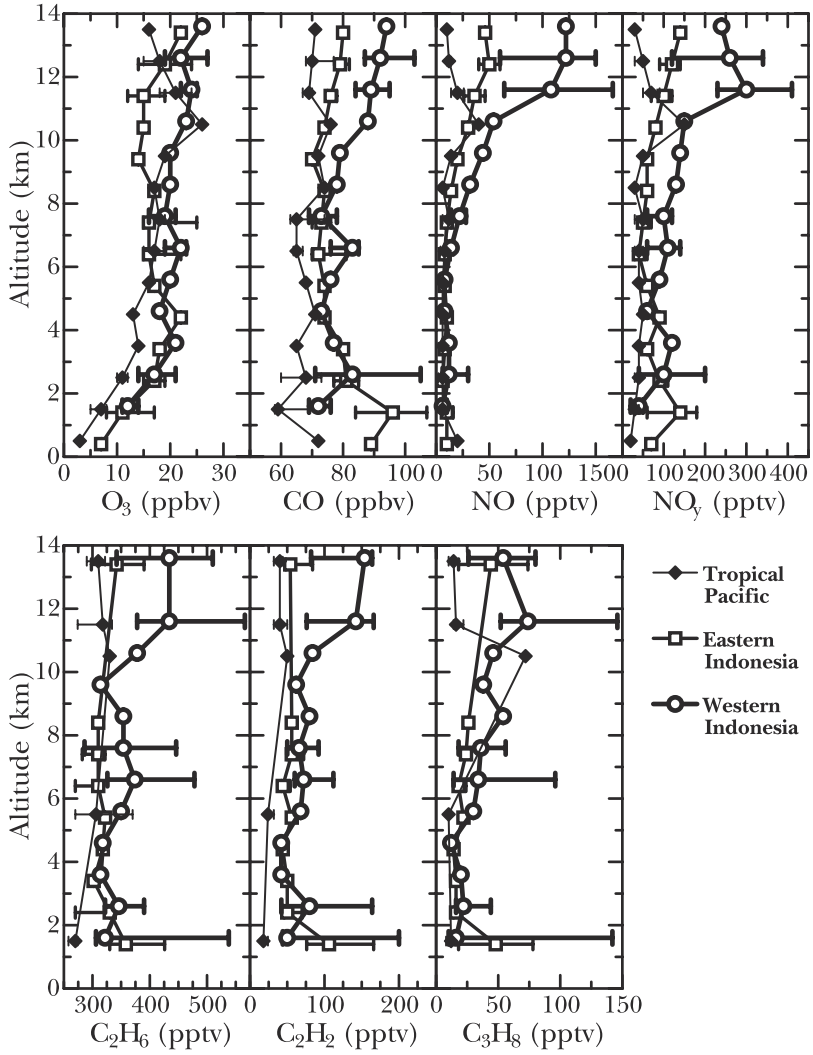

Figure 3. Altitude profiles of median values of O_3, CO, NO, NO_y, C_2H_6, C_2H_2, and C_3H_8 mixing ratios observed over the tropical Pacific Ocean (solid diamonds), eastern Indonesia (open squares), and western Indonesia (open circles). Bars indicate the central 50% of the range at selected altitudes.

probably insignificant because Tbb fell below the air temperature by more than 2–6 K in most encounters. Because each trajectory calculated using the ECMWF data cannot fully express air motion disturbed by convection, only statistical results are used in this analysis. The fractional distribution of the time from the latest encounters of air masses with optically thick clouds to the sampling of the air masses is shown in Figure 6. Over the tropical Pacific Ocean, eastern Indonesia, and western Indonesia, most air masses encountered optically thick clouds within 24–48 hours prior to the observation. Namely, most air masses in the upper troposphere over Indonesia frequently encountered cumulus convection over Indonesia during BIBLE-A, similar to the air masses over the tropical Pacific Ocean near the Intertropical Convergence Zone (ITCZ), suggesting that most air masses in the upper troposphere were repeatedly influenced by cumulus convection during their passage over Indonesia.

[14] These results, including those in section 3.1, show that the increase of ozone precursor concentrations in the upper troposphere over this region was attributed to convection effects: mixing with lower tropospheric air and NO production by lightning. It is likely that the much higher mixing ratios of ozone precursors over western Indonesia were due in part to the accumulation of this convective effects. They could also be attributed to more intense anthropogenic sources in western Indonesia because the population and anthropogenic activities in Java Island and Sumatra Island are much higher than those in other islands in Indonesia.

[15] However, the above conclusion is apparently inconsistent with the lower median mixing ratios of C_2H_6, C_2H_2, and C_3H_8 in the lower troposphere over Indonesia than those above 10 km over western Indonesia, although their central 50% ranges in the upper and lower troposphere were similar (Figure 3). Lower tropospheric air samples over Indonesia were obtained over several limited areas including near or over the ocean during BIBLE-A as shown in section 3.3.1 (Figure 7), and the lower median values in the lower troposphere were likely due to the larger percentage of clean air in the lower tropospheric air samples than that in the average lower tropospheric air over Indonesia. The lower median values in the lower troposphere were also

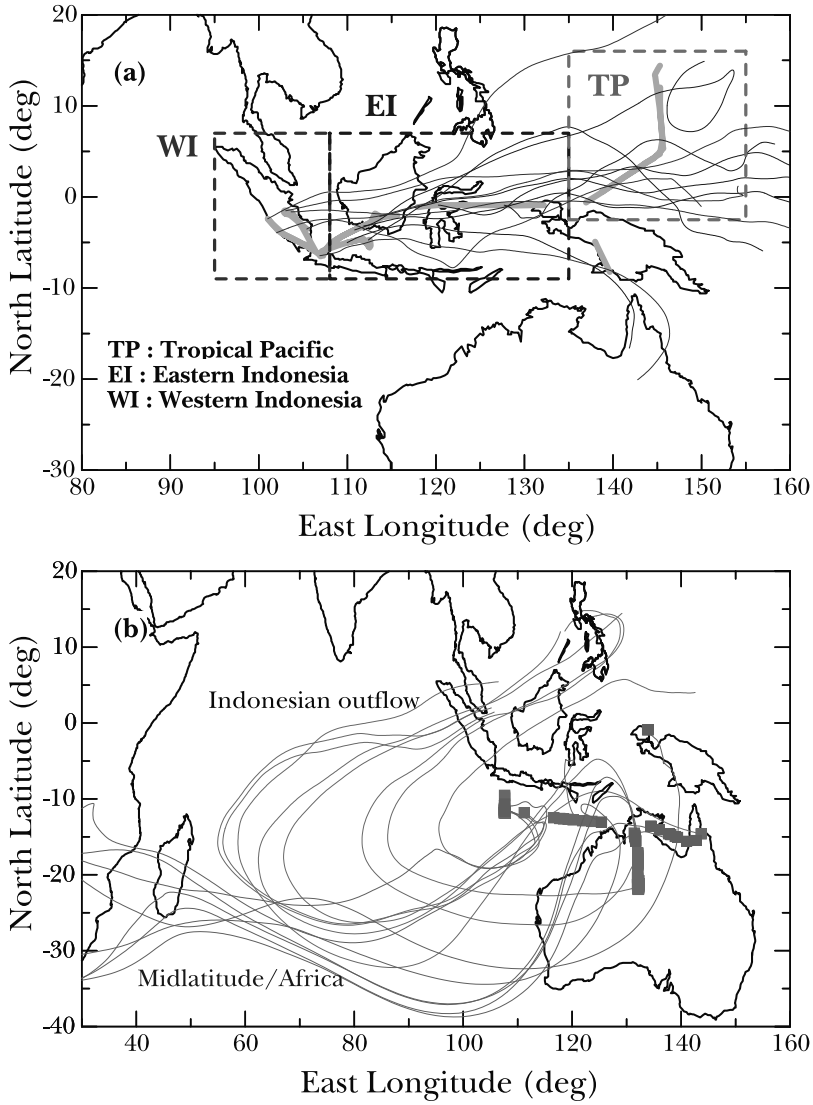

Figure 4. (a) Aircraft flight tracks (gray curves) above 8 km over the tropical Pacific Ocean (shown by box 'TP'), eastern Indonesia (shown by box 'EI'), and western Indonesia (shown by box 'WI') during BIBLE-A. Examples of backward trajectories from the flight tracks over eastern and western Indonesia are shown by blue and red curves, respectively. (b) Examples of backward trajectories (thin curves) from the observation points (squares) for the Indonesian outflow air (orange) and the midlatitude/African air (light blue). See color version of this figure at back of this issue.

partly due to several clean free-tropospheric air samples included in the lower tropospheric data, because the top height of the boundary layer, determined from the temperature profiles, varied from 1.5 km to 3.5 km over Indonesia during BIBLE-A.

3.3. Sources of Ozone Precursors

[16] Sources of ozone precursors over Indonesia were investigated by comparing correlations among ozone precursors in the upper troposphere with those in the lower troposphere (below 3 km), where the sampled air was influenced by surface sources (see Figure 3).

3.3.1. Correlations in the Lower Troposphere

[17] Air masses influenced by urban pollution and/or biomass burning were sampled in the lower troposphere in areas A, B, and C shown in Figure 7. In the Bandung-Jakarta area (area A), air masses with NO_y mixing ratios exceeding 200 pptv were often sampled in the lower troposphere. Because this area is the most densely populated area in Indonesia, this air was presumably polluted by fossil fuel combustion and burning of agricultural waste. The polluted air was also sampled near the Balikpapan airport (area C) in east Kalimantan. The data from areas A and C are referred to as urban area data. Biomass burning in Indonesia was nearly inactive during BIBLE-A, and air obviously affected by biomass burning was sampled only at a wood-burning area in south Kalimantan (area B). The data from area B are referred to as biomass burning area data.

[18] Lower tropospheric air was also sampled over the ocean around Indonesian islands (areas a and c in Figure 7) or over forests in middle Sumatra Island (area b). The

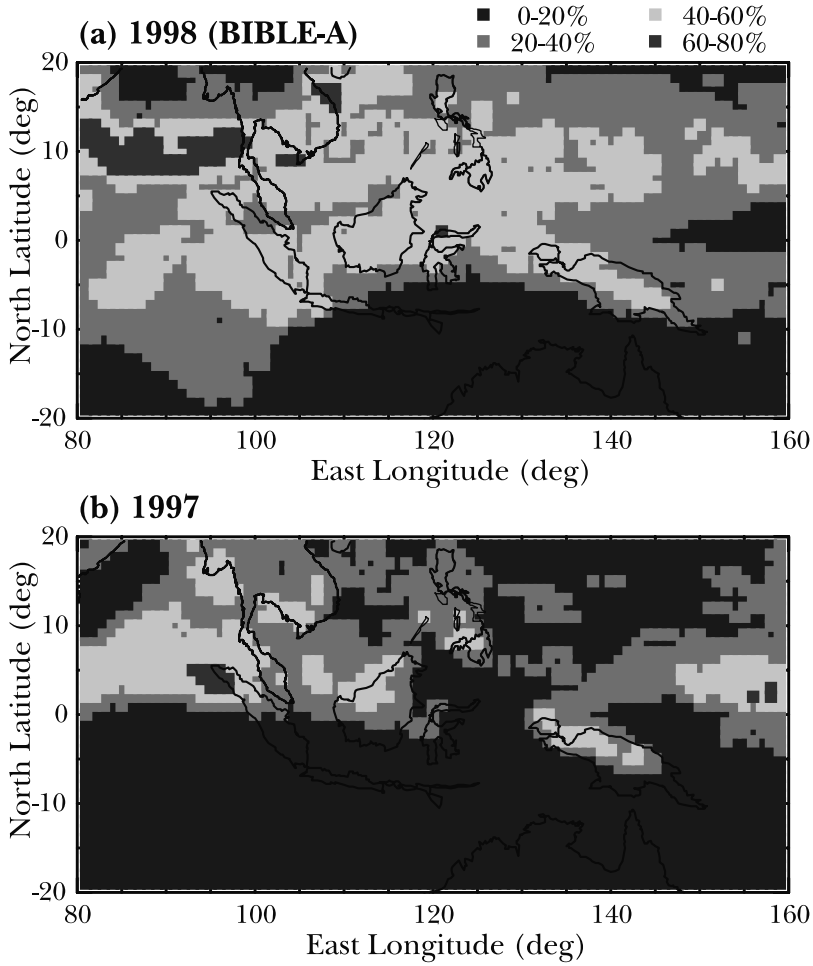

Figure 5. Occurrence distribution of high (>8 km), optically thick clouds in the Indonesian region between 24 September and 10 October in (a) 1998 and (b) 1997. See color version of this figure at back of this issue.

mixing ratios of NO_y and CO in these areas were mostly lower than 150 pptv and 90 ppbv, respectively, suggesting that there was no significant source of ozone precursors nearby. The data obtained in these areas are referred as the background area data.

[19] Figures 8a–8e are scatterplots of the mixing ratios of NO_y, C_2H_2, C_2H_4, C_2H_6, and CH_3Cl versus the CO mixing ratio in the lower troposphere over Indonesia. Although the data are scattered, the mixing ratios of these species were positively correlated with CO. Differences in these correlations were due to different sources of these species and/or dilution by the air from the background area (background air). A linear regression line (thin line) is fit to the background area data in Figures 8a–8e. Correlations of these species in the biomass burning area data are similar to those in the background area data, suggesting that the biomass burning plumes were rapidly diluted with the background air. In Figure 8a, the urban area data can be divided into two groups: high-NO_y data (>240 pptv), which are distributed significantly above the background area data lines, and low-NO_y data (<240 pptv), which are more similar to the background area data. The high-NO_y data were likely affected by urban pollution while the low-NO_y data were significantly diluted with the background air. In Figures 8b–8d, the mixing ratios of C_2H_2, C_2H_4, C_2H_6, and CO in the high-NO_y data were generally higher than the other data. A thick line is fit to the high-NO_y data in each figure to represent the correlation in the urban polluted air.

[20] CH_3Cl is considered a good biomass burning tracer [e.g., *Andreae et al.*, 1996; *Blake et al.*, 1996b, 1999; *Shirai et al.*, 2002]. Figure 8e shows that its mixing ratio was relatively high and clearly correlated with the CO mixing ratio both in the biomass burning area data and in the background area data. This result suggests that biomass burning (including forest fires, burning of agricultural waste, and wood fuel combustion) was a dominant source of ozone precursors in the background areas, although biomass burning was nearly inactive in Indonesia during BIBLE-A. The slope ($\Delta CH_3Cl/\Delta CO$) value of 2.1 pptv/ppbv in the background area and biomass burning area data is higher than that reported in Africa, Brazil, and northern Australia [e.g., *Blake et al.*, 1996b; *Shirai et al.*, 2002], suggesting higher Cl concentration in burnt biomass and/or lower combustion efficiency (smoldering) in biomass burning during BIBLE-A. In contrast, the slope value of 0.9 pptv/ppbv in the high-NO_y data is significantly smaller than that in the background area data.

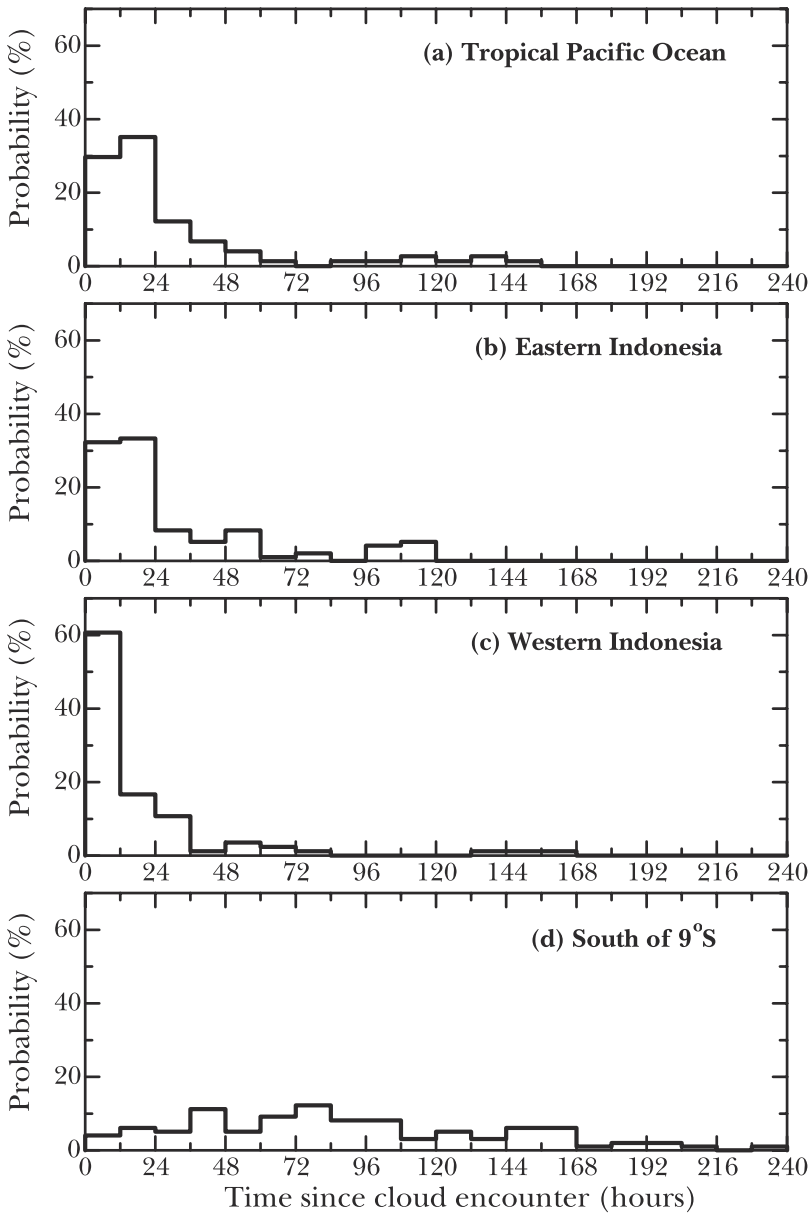

Figure 6. Fractional distribution of time from the latest encounter of the observed air masses with clouds to the observation in (a) the tropical Pacific area, (b) eastern Indonesia area, (c) western Pacific area, and (d) south of 9°S.

CH_3Br, which was positively correlated with CO in the air affected by biomass burning plumes [e.g., *Blake et al.*, 1996b, 1999; *Shirai et al.*, 2002], was not correlated with CO in the urban area data (not shown). These results suggest that biomass burning was not a dominant contributor to the increase of NO_y, CO, and NMHCs in the urban areas.

3.3.2. Source of Ozone Precursors in the Upper Troposphere

[21] Figures 9a–9d are scatterplots of the mixing ratios of C_2H_2, C_2H_4, C_2H_6, and CH_3Cl versus CO in the upper troposphere over eastern and western Indonesia. The background area data line (thin line) and the high-NO_y data line (thick line) in the lower troposphere (Figures 8b–8e) are also shown for comparison. The upper tropospheric data are mostly distributed between these lines. This distribution likely resulted from mixing of air masses from the urban, biomass burning, and background areas during upward transport from the lower troposphere due to convection. Chemical destruction of CO, C_2H_2, C_2H_6 and CH_3Cl was negligible, because their chemical lifetime is much longer than the typical time since the emission of CO and NMHCs from their sources till the air sampling (a few days). Dilution by middle tropospheric air over Indonesia and upper tropospheric air from the tropical Pacific Ocean would also occur during transport, and the dilution effect should be similar to that by lower tropospheric background air, except for CH_3Cl, because the mixing ratios of CO, NMHCs were similar in these air masses. The dilution effect

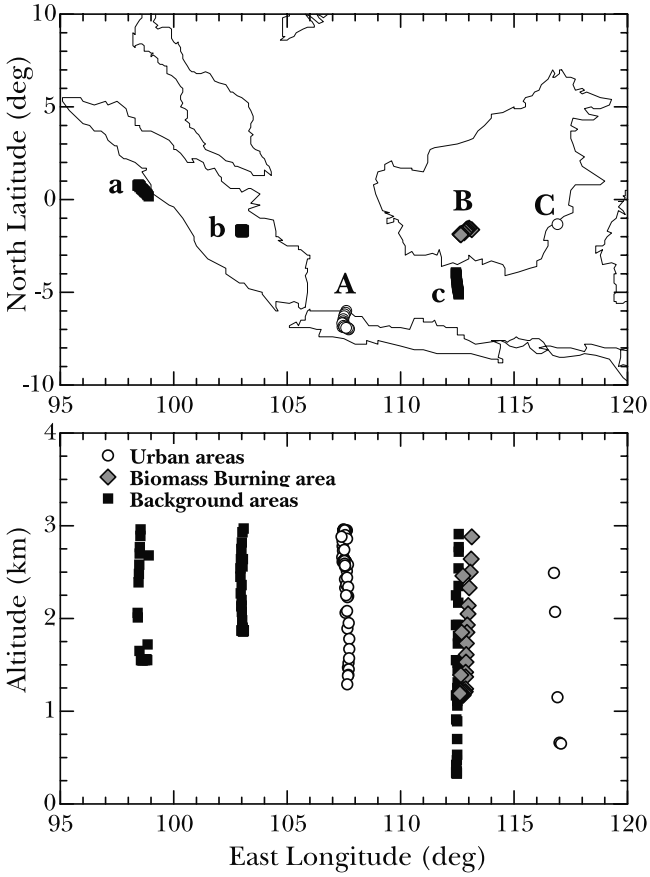

Figure 7. Sampling location of lower tropospheric air over Indonesia: (top) longitude-latitude cross section and (bottom) longitude-altitude cross section.

for CH_3Cl should decrease its concentration more largely in comparison with that by the lower tropospheric background air because of its low concentration in the middle and upper tropospheric air.

[22] The CO-C_2H_2 pair had one of the tightest correlations during BIBLE-A. In Figure 9a, data in the upper troposphere are distributed near the background data line, indicating that urban-polluted air was largely diluted. If the most of the lower tropospheric air transported to the upper troposphere were the background and/or biomass burning area air, the CH_3Cl mixing ratio should be high and should correlate with the CO mixing ratio, as shown by the background data line. However, the CH_3Cl concentration did not correlated with CO in the upper troposphere (Figure 9d). This result shows that both urban pollution and biomass burning contributed as the source of CO and NMHCs.

[23] In Figure 9c, the C_2H_6 mixing ratio in several air samples over eastern and western Indonesia greatly exceeds the high-NO_y data line (thick line) in the lower troposphere. These data require additional considerations. Such a high C_2H_6 mixing ratio compared with CO was not observed in the areas where lower tropospheric air was sampled during BIBLE-A (Figure 7). Similar results were obtained for C_3H_8, n-C_4H_{10}, and i-C_4H_{10} (not shown), suggesting that additional sources of light alkane species existed elsewhere in Indonesia. Emission or leakage of natural gas is a possible source, considering that the mining of natural gas, coal, and petroleum is widespread in Indonesia.

[24] Figure 3 shows that the central 50% range of the NO_y mixing ratio in the upper troposphere over western Indonesia was much higher than that in the middle and lower troposphere. The NO_y mixing ratios were often enhanced without discernable CO increases in the upper troposphere over Indonesia (see Figure 8a of *Koike et al.* [2002]). These results suggest that an additional, noncombustion source contributed to the increase of NO_y in the upper troposphere. *Koike et al.* [2002] concluded that lightning discharges, which often occurred over Indonesia during BIBLE-A, were probably the major source of NO and NO_y in the upper troposphere over Indonesia. Lightning flash rates detected by the Lightning Image Sensor (LIS) usually exceeded 50 per day per $1^\circ \times 1^\circ$ area over Java Island, Sumatra Island and south Kalimantan during BIBLE-A. *Koike et al.* [2002] estimated that the contribution of lightning-produced NO_x and NO_y was about 80% (40–60 pptv) and 50% (70–100 pptv), respectively, in the upper troposphere over Indonesia.

[25] In the middle troposphere between 4 and 8 km, the observed mixing ratios of ozone precursors were generally low over Indonesia, as shown in Figure 3; the CO and NO_y mixing ratios were mostly lower than 85 ppbv and 150 pptv, respectively. However, when the G-II aircraft entered cumulus clouds in the middle troposphere, mixing ratios of ozone precursors increased greatly, suggesting that polluted air was transported upward in the cumulus clouds. For example, on 6 October (flight 10), when the G-II aircraft entered towering cumulus clouds at about 7 km over Java Island, the mixing ratios of CO, C_2H_4, C_2H_6, and NO_y increased from ~70 ppbv, ~30 pptv, ~310 pptv, and ~170 pptv to ~150 ppbv, ~260 pptv, ~580 pptv, and ~750 pptv, respectively. This result suggests that polluted lower tropospheric air was transported into the upper troposphere by convection and was not released from the cumulus clouds in the middle troposphere [e.g., *Wang et al.*, 1996].

3.4. Ozone Formation in Indonesian Outflow

[26] The Indonesian outflow air masses, which were transported from western Indonesia via the Indian Ocean, were observed in the upper troposphere south of 9°S over the ocean south of Indonesia and over northern Australia (Figure 4b). The data sampling the Indonesian outflow air accounted for about 60% of the total number of data obtained in this region. As shown in Figure 6d, most of the Indonesian outflow air masses were transported to the observation points without the influence of convection after they left Indonesia. Figure 10 shows the probability distributions of the NO_y mixing ratio in the tropical Pacific Ocean, eastern Indonesia, western Indonesia, Indonesian outflow air, and midlatitude/African air. It should be noted that the distribution in the Indonesian outflow air is quite similar to that in western Indonesia but largely different from that in midlatitude/African air, although both air masses were observed south of 9°S. The mixing ratios of NO, NO_y, CO, C_2H_6, C_2H_2, and C_3H_8, except for C_2H_4, in the Indonesian outflow air were also similar to, but slightly smaller than, those in western Indonesia, as shown in

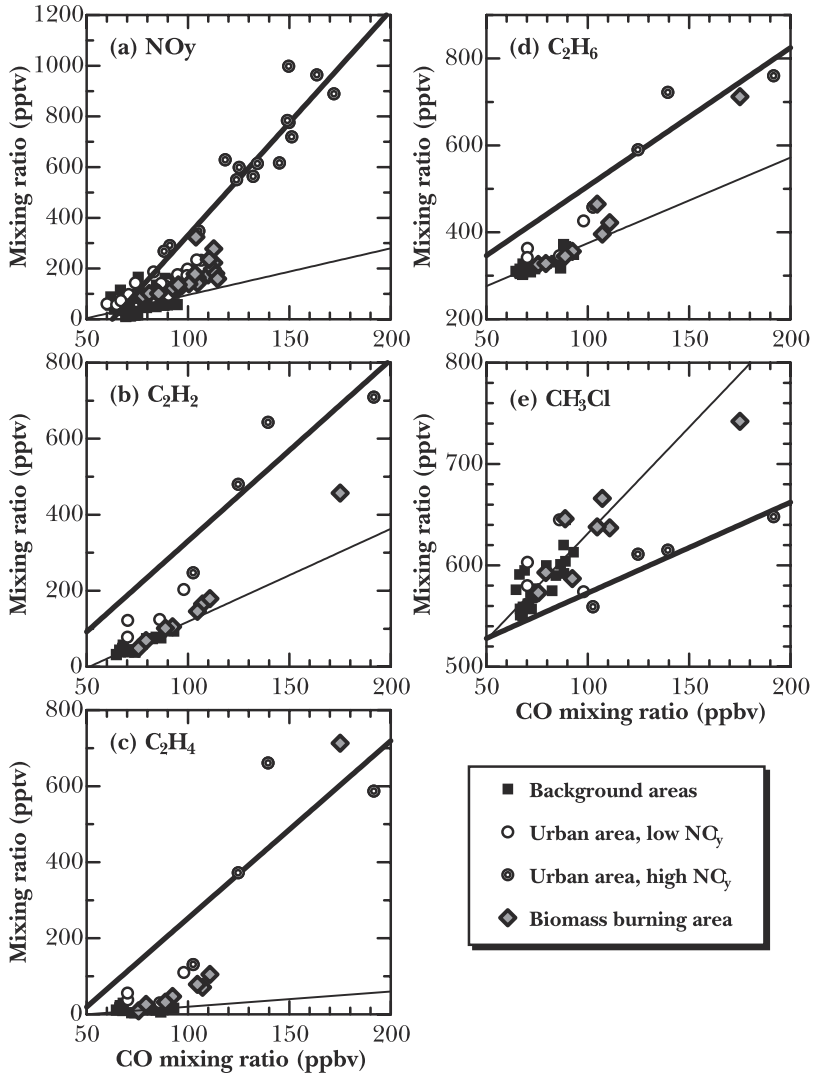

Figure 8. Correlation of (a) NO_y, (b) C_2H_2, (c) C_2H_4, (d) C_2H_6, and (e) CH_3Cl with CO in the lower troposphere over Indonesia. Thin lines are fit to the data obtained in the background areas, and thick lines are fit to the high-NO_y data obtained in the urban areas.

Figures 2b–2h. This similarity in the distribution of these ozone precursors between the Indonesian outflow air and western Indonesian air is consistent with the backward trajectories, confirming that the Indonesian outflow air originated in western Indonesia. The lower mixing ratio of C_2H_4 in the Indonesian outflow air (Figure 2f) is reasonable considering its chemical lifetime (a few days), which is shorter than the time for transport from western Indonesia (4–9 days).

[27] As shown in Figure 2a, while the ozone concentration over eastern Indonesia (median 18 pptv) and western Indonesia (22 pptv) are similar to that over the tropical Pacific Ocean (17 ppbv), that in the Indonesian outflow air was significantly higher (33 ppbv). Figures 11a and 11b are scatterplots of ozone mixing ratios versus NO and NO_y mixing ratios in the western Indonesian and Indonesian outflow air, respectively. The ozone mixing ratio did not increase significantly with the NO and NO_y mixing ratios in western Indonesia, although they were positively correlated. In contrast, the ozone mixing ratio increased noticeably with NO and NO_y in the Indonesian outflow air, although the scatter of data was large for NO (Figure 11b).

[28] We interpret these results as the progress of the photochemical ozone formation during transport. The diurnally averaged ozone formation rate ($F(O_3)$) and destruction rate ($D(O_3)$) were estimated for every 1-minute data average by using a photochemical box model [*Kotamarthi et al.*, 1997; *Ko et al.*, 2002] constrained by the observed mixing ratios of ozone, H_2O, CH_4, NO, NO_y, and NMHCs. As shown in Table 2, where median values of $F(O_3)$, $D(O_3)$, and $F(O_3)$-$D(O_3)$ are listed, the model showed that net photochemical ozone formation occurred in all air mass categories in the upper troposphere. The median $F(O_3)$-$D(O_3)$ value was less than 1 ppbv/d in the tropical Pacific Ocean and eastern Indonesia. This value suggests a small ozone increase of 1–2 ppbv during transport from the tropical Pacific Ocean to western Indonesia, because the average transport time from 140°E (tropical Pacific Ocean) to 108°E (boundary between eastern and western Indonesia) was 2.6 days in the upper troposphere. Because the ozone

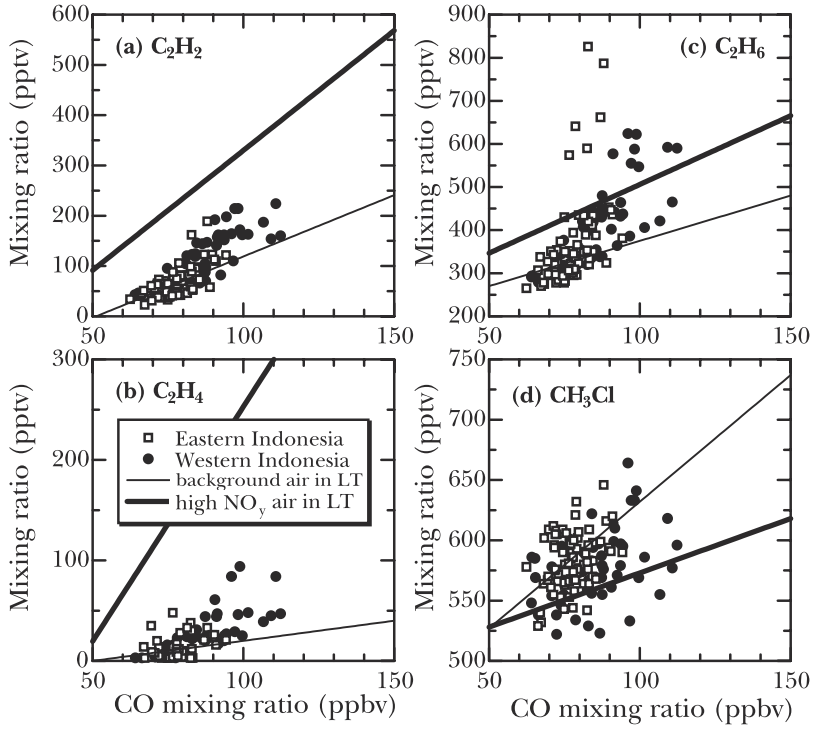

Figure 9. Correlation of (a) C_2H_2, (b) C_2H_4, (c) C_2H_6, and (d) CH_3Cl with CO in the upper troposphere over eastern and western Indonesia. The lines fit to the background area data and high-NO_y data in the lower troposphere are also shown for comparison.

mixing ratios in the lower troposphere were generally low (Figure 3), consistent with the small or negative ozone formation rates estimated by the model, upward transport did not increase ozone in the upper troposphere over western Indonesia. Because of high NO mixing ratios, the model estimated high net ozone formation rates of 2.1 ppbv/d (median) over western Indonesia. However, considering that the high NO_x mixing ratios were mostly caused by lightning influence within 24–48 hours prior to the observation [*Koike et al.*, 2002], the expected ozone increase was not large over this region. These results indicate that the small ozone increase in this region was consistent with the model result, considering insufficient time elapsed since the increase of ozone precursor concentrations. Based on the ozone increase of 11 ppbv (median) in the Indonesian outflow air and the average transport time of 6 days from the western border of the western Indonesia area to the observation points, the average net ozone formation rate during transport from western Indonesia is estimated to be 1.8 ppbv/d. This value is consistent with the model estimation: between 1.4–3.0 ppbv/d over western Indonesia and 0.8–1.5 ppbv/d in the Indonesian outflow air.

[29] Figure 12 illustrates photochemical ozone production in the air masses affected by convection over Indonesia. *Jacob et al.* [1996] proposed that deep convection over South America, southern Africa, and Oceania injects NO_x from combustion including biomass burning, soils, and lighting into the upper troposphere, leading to ozone production. We illustrated similar processes over Indonesia and also included ozone production during horizontal transport over the Indian Ocean. *Jacob et al.* [1996] estimated the diurnally averaged net ozone formation rate at 8–12 km was 2.1 ppbv/d (median) over the South Atlantic basin during the Transport and Atmospheric Chemistry near the Equator-Atlantic (TRACE-A) experiment in September–October 1992. *Schultz et al.* [1999] also estimated it to be 1–1.5 ppbv/d (median) over the tropical South Pacific during Pacific Exploratory Mission (PEM)-Tropics A experiment in September–October 1996. These net ozone formation rate values are similar to those over the western Indonesia and in the Indonesian outflow air during BIBLE-A, showing that the convection influence on the ozone production in the upper troposphere over Indonesia (mainly through NO_x production by lightning) was comparable to the effect by biomass burning in Africa and South America. *Pickering et al.* [1993] suggested that lightning-produced NO_x was the greatest factor increasing ozone formation in association with the convection around northern Australia during the Equatorial Mesoscale Experiment (EMEX) and the Stratosphere-Troposphere Exchange Project (STEP) in February 1987, when biomass burning was inactive in this region. They suggested that lightning over northern Australia increased the ozone formation rate by 2–3 times to 1.2–1.4 ppbv/d at 12–14 km, comparable to but smaller than that over western Indonesia during BIBLE-A.

[30] Advection of air masses from the tropical Pacific Ocean to the south subtropical Pacific Ocean via Indonesia, the Indian Ocean, and northern Australia in the upper troposphere commonly occurs from June–July to November–December, and active convection over Southern Hemispheric Indonesia, especially over western Sumatra Island, occurs from September to March. Hence it is likely that convection over Indonesia brings the ozone precursors up from the surface or produces NO by lightning to increase

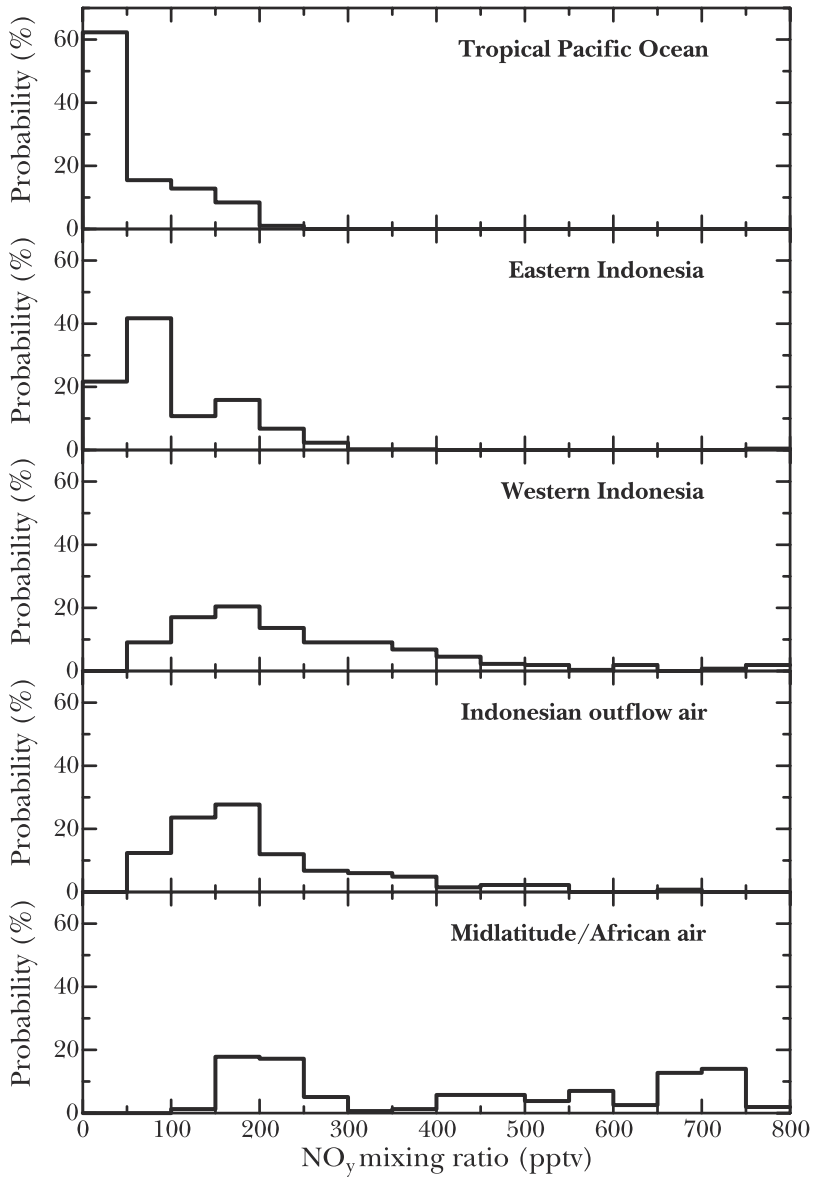

Figure 10. Probability distribution of NO_y mixing ratio in the upper troposphere in each air mass category.

the ozone mixing ratio in the upper troposphere over the Indian Ocean, northern Australia, and the south subtropical Pacific Ocean from September to December. During PEM-Tropics A, which was conducted from August to October 1996 during a La Niña period, the air masses passing over Indonesia were observed over the south subtropical Pacific Ocean near Fiji (18°S, 178°E) [*Board et al.*, 1999]. The median ozone mixing ratio observed in these air masses was higher (46 ppbv) than that for the air masses transported from the ITCZ region (28 ppbv). Convection over Indonesia likely contributed to this higher ozone mixing ratio.

4. Summary and Conclusions

[31] Distributions of ozone and its precursors were observed over Indonesia and northern Australia between 24 September and 10 October 1998. The observations were carried out during the transition period from dry season to wet season in Indonesia, and convection was very active over Indonesia during this period due to the prevailing La Niña condition. Over the tropical Pacific Ocean, the mixing ratios of ozone and its precursors were low. Over Indonesia, the ozone mixing ratio was also low (~20 ppbv) throughout the troposphere, and significantly lower than the 5-year average ozone mixing ratio observed by ozonesondes in Indonesia from August to November [*Fujiwara et al.*, 2000]. However, simultaneous increases of NO, NO_y, CO, and NMHCs mixing ratios were frequently observed over Indonesia, especially in western Indonesia. The increase of ozone precursors was confined to the upper troposphere above 8 km.

[32] The increase of ozone precursors over Indonesia in the upper troposphere is attributed to the influence of active convection in this region because: (1) air masses in the

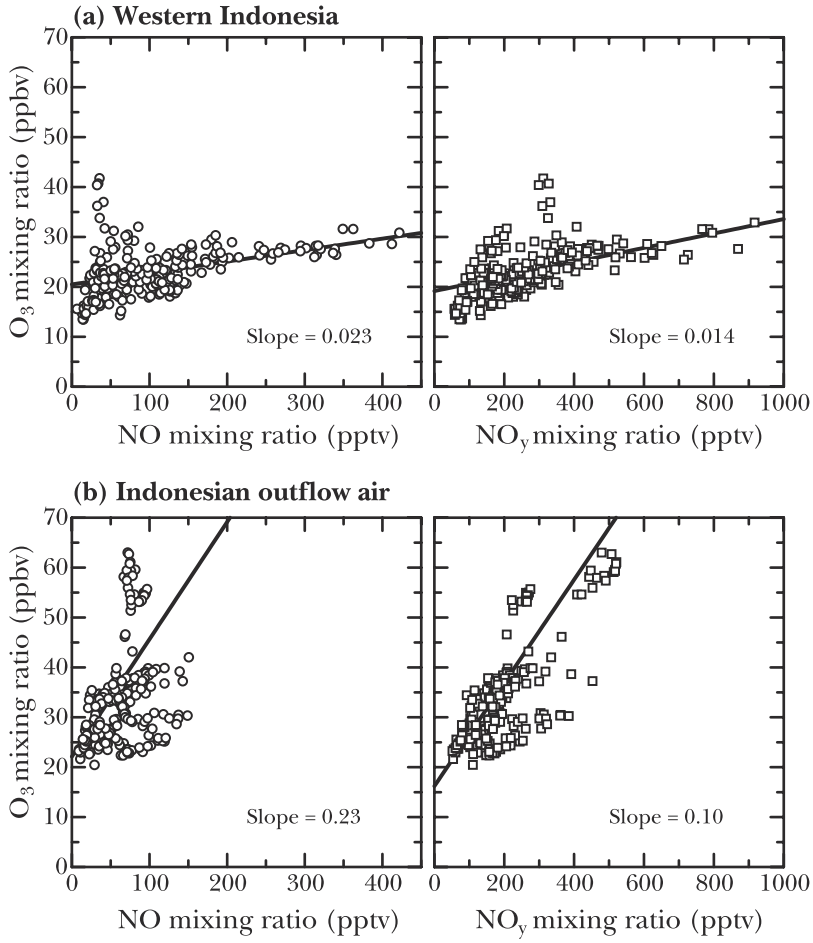

Figure 11. Scatterplots of ozone versus NO and NO_y in the upper troposphere (a) over western Indonesia and (b) in the Indonesian outflow air. The slope value for the straight line fit to the data points is shown in each panel.

upper troposphere over Indonesia were transported from the east (tropical Pacific Ocean) to the west (western Indonesia), and the mixing ratios of ozone precursors increased along this transport direction, (2) higher concentration of several short-lived NMHCs, such as C_2H_4, indicate that the air masses were influenced by emissions from surface sources within a few days prior to the observation, and (3) a meteorological analysis using backward trajectory and GMS-5 IR cloud image data shows that most air masses observed over Indonesia had encountered optically thick (probably cumulus) clouds within 24–48 hours prior to the observation. Comparison of the correlation between CO and NMHCs in the upper troposphere with that in the lower troposphere shows that the increase of these species in the upper troposphere can be explained as the result of the convective transport of polluted air observed in the lower troposphere over Indonesia. Biomass burning was nearly inactive during BIBLE-A. Correlation analysis of CH_3Cl with CO indicates that both urban pollution, probably including fossil fuel combustion and the burning of agricultural waste, and biomass burning were sources of CO and NMHCs during BIBLE-A. *Koike et al.* [2002] showed that

Table 2. Median Values of Diurnal Average Ozone Formation Rate ($F(O_3)$), Ozone Destruction Rate ($D(O_3)$), and Net Ozone Formation Rate (Net $F(O_3)$) Calculated for the Tropical Pacific Ocean, Eastern Indonesia, Western Indonesia, Indonesian Outflow Air, and Midlatitude/African Air[a]

	$F(O_3)$	$D(O_3)$	Net $F(O_3)$
Tropical Pacific Ocean	0.42 −0.10/+0.35	0.18 −0.05/+0.05	0.33 −0.10/+0.30
Eastern Indonesia	1.02 −0.25/+0.45	0.28 −0.15/+0.35	0.68 −0.25/+0.40
Western Indonesia	2.53 −0.65/+0.85	0.38 −0.20/+0.45	2.08 −0.65/+0.90
Indonesian outflow air	1.33 −0.30/+0.30	0.23 −0.05/+0.10	1.18 −0.35/+0.30
Midlatitude/African air	1.72 −0.25/+0.20	0.33 −0.10/+0.10	1.33 −0.10/+0.15

[a] The units are ppbv/d. The central 50% of the range is also shown.

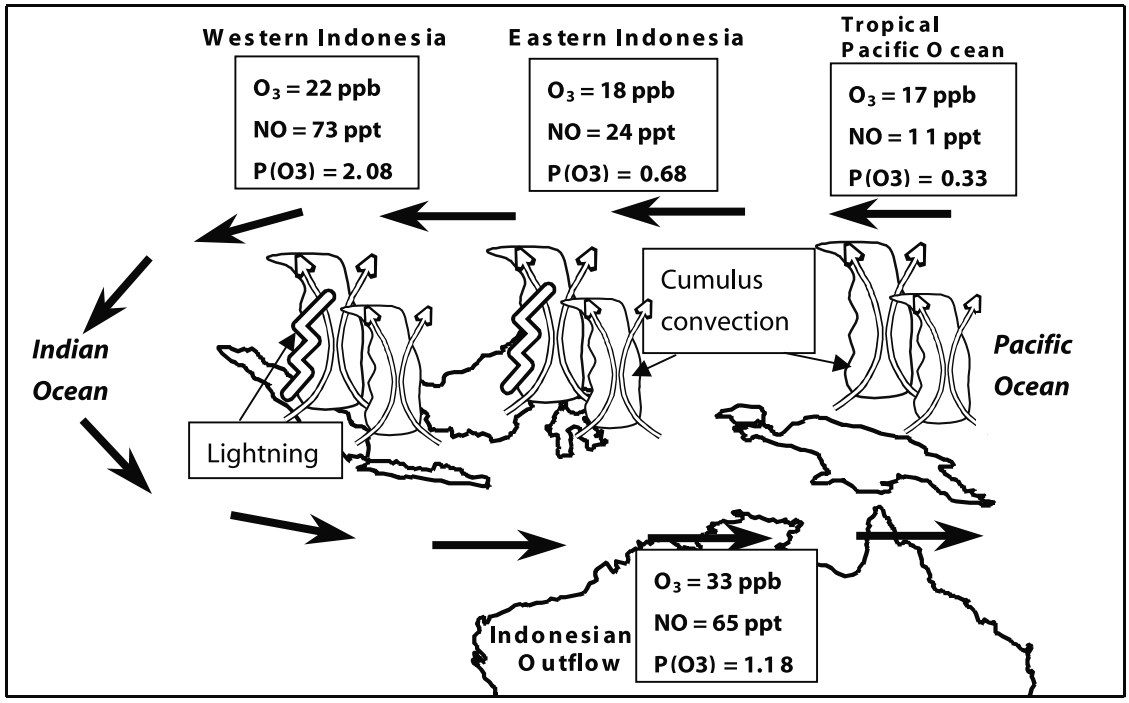

Figure 12. Schematic of the influence of the convection over Indonesia on photochemical ozone production in the upper troposphere. Horizontal advection in the upper troposphere is shown by black arrows, and upward transport is shown by white arrows. Median values of the mixing ratios of NO and ozone and the net ozone production rate (in ppbv/d) are shown in boxes for the tropical Pacific Ocean, eastern Indonesia, western Indonesia, and Indonesian outflow air masses.

lightning associated with convection activity mainly contributed to the observed increase of NO and NO_y in the upper troposphere.

[33] The increase of ozone precursors due to convection over Indonesia led to net photochemical ozone production. Because of the short time elapsed since the increase of ozone precursors, the increase in ozone concentration was limited over Indonesia. Backward trajectories show that about 60% of the air samples over the ocean south of Indonesia and over northern Australia during BIBLE-A were identified as Indonesian outflow air, which was transported from western Indonesia to northern Australia via the Indian Ocean. In these air masses, the mixing ratios of ozone precursors, except for the short-lived species, were similar to, but slightly smaller than, those in western Indonesia, consistent with the trajectory analysis. Only the ozone mixing ratio was significantly higher (median 33 ppbv) in the Indonesian outflow air compared with that in the air over western Indonesia (median 22 ppbv), and it was also positively correlated with NO and NO_y. These results indicate photochemical ozone production during transport. Considering the transport time (average 6 days), the average ozone formation rate was estimated to be 1.8 ppbv/d. This value was similar to the net, diurnally averaged ozone formation rate estimated by using a photochemical model for the air over western Indonesia (1.4–3.0 ppbv/d) and for the Indonesian outflow air (0.8–1.5 ppbv/d), and compared with that in air masses affected by biomass burning in Africa and South America during TRACE-A and PEM Tropics-A [*Jacob et al.*, 1996; *Schultz et al.*, 1999].

[34] This study demonstrates that active convection over Indonesia carries ozone precursors to the upper troposphere, and that a discernable increase in ozone mixing ratio occurred over the Indian Ocean and northern Australia, although there was little biomass burning activity in 1998, during a La Niña period. Convection over Indonesia and transport of air masses in the upper troposphere over Indonesia to the south subtropical Pacific Ocean via the tropical Indian Ocean and northern Australia generally occur during the September–December period. Therefore it is likely that ozone increases in the upper troposphere during this period are caused by these processes that transport ozone precursors produced by biomass burning, urban pollution and lightning in Indonesia.

Appendix A

[35] Here the instruments for ozone and CO measurements and the scaling of $J(NO_2)$ and $J(O^1D)$ radiometer data are described.

[36] The ozone mixing ratio was measured by using a dual-beam UV-absorption ozone photometer, which was newly developed by the University of Tokyo and Dylec Co. (Ibaraki, Japan). By adopting the dual-beam configuration [*Proffitt and McLaughlin*, 1983] and reducing dead volume, both the time response and the dead time for taking reference (zero-ozone) signals was improved to 1 s above an altitude of 2.5 km and 2 s below 2.5 km. The length of each absorption cell is 76 cm, and the temperatures of the absorption cells and a low-pressure mercury lamp are

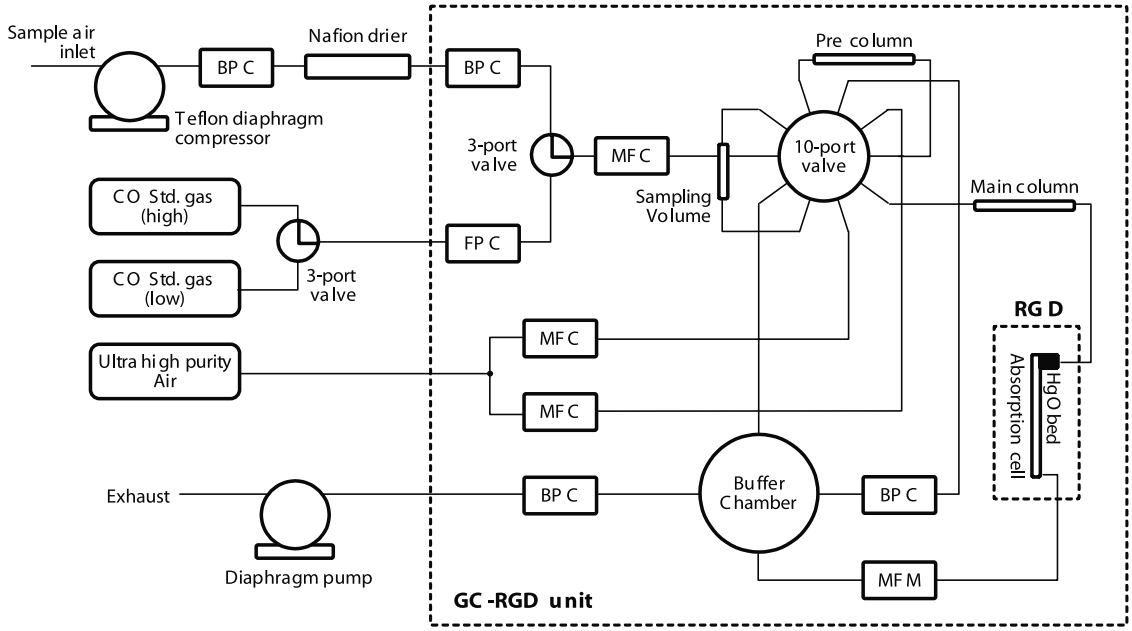

Figure A1. Diagram of the GC-RGD instrument for measuring CO. One of four GC-RGD units is shown. Optics and electronics are omitted. BPC, back pressure controller; FPC, forward pressure controller; MFC, mass flow controller; MFM, mass flowmeter.

regulated to minimize fluctuation and drift in lamp intensity and cell transmittance. UV-enhanced silicon photodiodes with a thermoelectric cooler and voltage-frequency converters synchronized to a crystal oscillator are used to reduce thermal and electronic noise. The signal and housekeeping data (the pressure and temperature of each cell and the mass flow rate of sample air) are recorded by a microcomputer at a time interval of 1 second. The ozone instrument was calibrated in the laboratory before and after the observation campaigns. The ozone mixing ratio can be derived from a simple equation: [Ozone mixing ratio (ppbv)] = [absorbance (%)]/{$(1.65 \pm 0.05) \times 10^{-6} \cdot$ [cell pressure (hPa)]}. The differences between the absorption cells are negligible. One standard deviation of the calibration coefficient is 3%, and overall accuracy of this instrument is estimated to be 5%. The average precision estimated from the signal fluctuation in the laboratory is ±350/[cell pressure (hPa)] ppbv. It is ±0.3 ppbv at the 950 hPa level (near ground surface) and ±2.0 ppbv at the 170 hPa level (about 12 km). However, because the optics of the instrument often over-heated during BIBLE-A missions due to high ambient temperatures, fluctuations and drift of the signal were larger than that in the laboratory. Thus we used a running mean of 10 data points obtained during 12 s for the mixing ratio value discussed in this paper. In the BIBLE-B campaign conducted in August–September 1999, the overheating problems were avoided so the precision was better than that in BIBLE-A and was similar to the laboratory values.

[37] The CO concentration was measured by using an automated gas chromatograph (GC) system with a reduction gas detector (RGD), which was newly developed by the University of Tokyo. The RGD detects CO molecules by UV absorption due to mercury vapor that is produced by the reaction of CO with heated (260°C) mercuric oxide [e.g., *Robbins et al.*, 1968; *Seiler*, 1974; *Novelli et al.*, 1991]. Figure A1 illustrates a schematic diagram of the airborne GC-RGD system. The GC is used to separate CO from other reduced gases such as hydrogen. The GC cycle time, which limits the time response of this instrument, was 80 s using short packed columns (Unibeads 1S, 65 cm + Molecular Sieve 5A, 65 cm) heated to 105°C. By alternating four independent GC-RGD units, the sampling interval of the CO measurement was 20 s. Flow rate and pressure at each inlet and exhaust port were regulated to stabilize the GC-RGD signal during observation flights. To compensate for a slight nonlinear response of the GC-RGD signal (peak height) to the CO mixing ratio [*Novelli et al.*, 1998], a calibration of this instrument was repeatedly carried out using CO standard gases with various CO mixing ratios before, during, and after the BIBLE campaigns. Considering the nonlinearity, the precision of this instrument is estimated to be ±3 ppbv in the range between 0 and 400 ppbv. The accuracy relies on that of the standard gases, whose CO mixing ratio is determined by gravimetric analysis and is estimated to be about 5%.

[38] $J(NO_2)$ and $J(O^1D)$ were measured by using $J(NO_2)$ and $J(O^1D)$ filter radiometers (Meteorologie Consult, Koenigstein, Germany) [*Junkermann et al.*, 1989; *Volz-Thomas et al.*, 1996]. Both radiometers consist of up-looking and down-looking optical units, which were installed on the top and bottom of the fuselage. The data sampling rate was 1 s^{-1}, and the precisions of the $J(NO_2)$ and $J(O^1D)$ filter radiometers were better than 3%. The $J(NO_2)$ radiometer was absolutely calibrated by Meteorologie Consult. We compared the $J(NO_2)$ and $J(O^1D)$ values obtained during BIBLE-A with those obtained by a spectroradiometer during the PEM-Tropics A [*Shetter and Müller*, 1999]. For the compar-

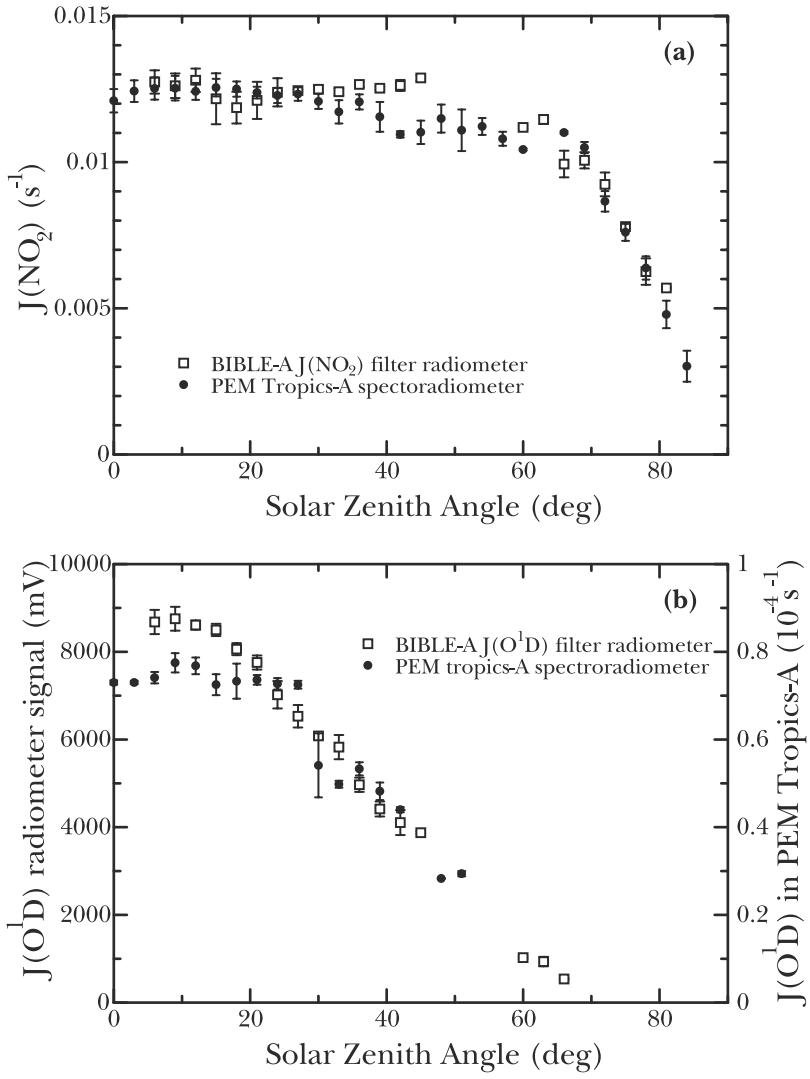

Figure A2. Comparison of (a) $J(NO_2)$ values and (b) $J(O^1D)$ radiometer signals in BIBLE-A with $J(NO_2)$ and $J(O^1D)$ values in PEM-Tropics A in the upper troposphere under clear-sky conditions. Bars show the range of ±1 standard deviation.

ison, only the data obtained during level flights above an altitude of 8.5 km were used. The total ozone range at the observation point was restricted to 250–280 DU using Total Ozone Mapping Spectrometer (TOMS) data, because the $J(O^1D)$ values are influenced by the overhead ozone column amount. Because the J-values are sensitive to cloud absorption and reflection, the cloud-affected data were excluded by using the aerosol surface area data and the ratio of up-looking/down-looking radiometer signals for the BIBLE-A data and by using the lidar aerosol data for the PEM-Tropics A data. Figure A2a compares the $J(NO_2)$ values in BIBLE-A with those in PEM Tropics-A, indicating that the $J(NO_2)$ values in BIBLE-A are similar to, but 3.5 ± 10% larger than those in PEM-Tropics A at the same solar zenith angle (between 6° and 52°). This comparison suggests that both observations are consistent with each other, considering the accuracy of each instrument (8% for both measurements). Figure A2b compares the signal values of the $J(O^1D)$ filter radiometer in BIBLE-A with the $J(O^1D)$ values in PEM Tropics-A. The $J(O^1D)$ radiometer signal in BIBLE-A mostly correlated with the $J(O^1D)$ values in PEM Tropics-A, although a systematic difference exists between the two values: the $J(O^1D)$ signal in BIBLE-A increased with decreasing solar zenith angle to 15°, while the PEM Tropics-A $J(O^1D)$ values were nearly constant with solar zenith angles less than 30°. The absolute sensitivity of the $J(O^1D)$ filter radiometer in BIBLE-A was determined by the linear fitting of its signal to the $J(O^1D)$ values in PEM-Tropics A. The deviation from the fit was less than 12% for solar zenith angles between 6° and 52°.

[39] **Acknowledgments.** This work is supported by NASDA as a part of the Global Atmospheric Chemistry Experiment (GLACE) of NASDA/EORC, and is also supported by the Japanese Ministry of Education, Science and Culture. The authors are indebted to all the participants for their cooperation and support, and thank the project office at NASDA/EORC and the flight crews at Diamond Air Service Co. for their assistance during the BIBLE-A campaign. The authors acknowledge T. Shirai (NASDA/EORC) for helpful discussions and thank M. Takeda (Kyoto

University) and Y. Ishikawa (University of Tokyo) for assisting us in the analysis of the data.

References

Andreae, M. O., et al., Methyl halide emissions from savanna fires in southern Africa, *J. Geophys. Res.*, *101*, 23,603–23,613, 1996.

Andreae, M. O., et al., Transport of biomass burning smoke to the upper troposphere by deep convection in the equatorial region, *Geophys. Res. Lett.*, *28*, 951–954, 2001.

Blake, D. R., T. Y. Chen, T. W. Smith Jr., C. J.-L. Wang, O. W. Wingenter, N. J. Blake, F. S. Rowland, and E. W. Mayer, Three-dimensional distribution of NMHCs and halocarbons over the northwestern Pacific during the 1991 Pacific Exploratory Mission (PEM WEST-A), *J. Geophys. Res.*, *101*, 1763–1778, 1996a.

Blake, N. J., D. R. Blake, B. C. Sive, T.-Y. Chen, F. S. Rowland, J. E. Collins, G. W. Sachse, and B. E. Anderson, Biomass burning emissions and vertical distribution of atmospheric methyl halides and other reduced carbon gases in the South Atlantic region, *J. Geophys. Res.*, *101*, 24,151–24,164, 1996b.

Blake, N. J., et al., Influence of southern hemispheric biomass burning on midtropospheric distributions of nonmethane hydrocarbons and selected halocarbons over the remote South Pacific, *J. Geophys. Res.*, *104*, 16,213–16,232, 1999.

Board, A. S., H. E. Fuelberg, G. L. Gregory, B. G. Heikes, M. G. Schultz, D. R. Blake, J. E. Dibb, S. T. Sandholm, and R. W. Talbot, Chemical characteristics of air from differing source regions during the Pacific Exploratory Mission-Tropics A (PEM-Tropics A), *J. Geophys. Res.*, *104*, 16,181–16,196, 1999.

Burrows, J. P., M. Weber, M. Buchwitz, V. Rozanov, A. Ladstätter-Weissenmayer, A. Richter, R. DeBeek, R. Hoogen, K. Bramstedt, K.-U. Eichmann, and M. Eisinger, The global ozone monitoring experiment (GOME): Mission concept and first scientific results, *J. Atmos. Sci.*, *56*, 151–175, 1999.

Chandra, S., J. R. Ziemke, W. Min, and W. G. Read, Effects of 1997–1998 El Niño on tropospheric ozone and water vapor, *Geophys. Res. Lett.*, *25*, 3867–3870, 1998.

Connors, V. S., B. B. Gormsen, S. Nolf, and H. G. Reichle Jr., Spaceborne observations of the global distribution of carbon monoxide in the middle troposphere during April and October 1994, *J. Geophys. Res.*, *104*, 21,455–21,470, 1999.

Crawford, J., D. Davis, G. Chen, R. Shetter, M. Muller, J. Barrick, and J. Olson, An assessment of cloud effects on photolysis rate coefficients: Comparison of experimental and theoretical values, *J. Geophys. Res.*, *104*, 5725–5734, 1999.

Folkins, I., R. Chatfield, D. Baumgardner, and M. Proffitt, Biomass burning and deep convection in southeastern Asia: Results from ASHOE/MAE-SA, *J. Geophys. Res.*, *102*, 13,291–13,299, 1997.

Fujiwara, M., K. Kita, S. Kawakami, T. Ogawa, N. Komala, S. Saraspriya, and A. Suripto, Tropospheric ozone enhancements during the Indonesian forest fire events in 1994 and in 1997 as revealed by ground-based observations, *Geophys. Res. Lett.*, *26*, 2417–2420, 1999.

Fujiwara, M., K. Kita, T. Ogawa, S. Kawakami, T. Sano, N. Komala, S. Saraspriya, and A. Suripto, Seasonal variation of tropospheric ozone in Indonesia revealed by 5-year ground-based observations, *J. Geophys. Res.*, *105*, 1879–1888, 2000.

Hauglustein, D. A., G. P. Brasseur, and J. S. Levine, A sensitivity simulation of tropospheric ozone changes due to the 1997 Indonesian fire emissions, *Geophys. Res. Lett.*, *26*, 3305–3308, 1999.

Inoue, T., On the temperature and effective emissivity determination of semi-transparent cirrus clouds by bi-spectral measurements in the 10 mm window region, *J. Meteorol. Soc. Jpn.*, *63*, 88–99, 1985.

Inoue, T., Features of clouds over the tropical Pacific during Northern Hemispheric winter derived from split window measurement, *J. Meteorol. Soc. Jpn.*, *67*, 621–627, 1989.

Jacob, D. J., et al., Origin of ozone and NOx in the tropical troposphere: A photochemical analysis of aircraft observations over the south Atlantic basin, *J. Geophys. Res.*, *101*, 24,235–24,250, 1996.

Junkermann, W., U. Platt, and A. Volz-Thomas, A photoelectric detector for the measurement of photolysis frequencies of ozone and other atmospheric molecules, *J. Atmos. Chem.*, *8*, 203–227, 1989.

Kawakami, S., et al., Impact of lightning and convection on reactive nitrogen in the tropical free troposphere, *J. Geophys. Res.*, *102*, 28,367–28,384, 1997.

Kita, K., M. Fujiwara, and S. Kawakami, Total ozone increase associated with forest fires over the Indonesian region and its relation to the El Niño-Southern Oscillation, *Atmos. Environ.*, *34*, 2681–2690, 2000.

Kley, D., P. J. Crutzen, H. G. J. Smit, H. Vomel, S. J. Oltmans, H. Grassel, and V. Ramanathan, Observation of near-zero ozone concentrations over the convective Pacific: Effects on air chemistry, *Science*, *274*, 230–233, 1996.

Ko, M., W. Hu, J. Rodriguez, Y. Kondo, M. Koike, K. Kita, S. Kawakami, D. Blake, and S. Liu, Photochemical ozone budget during the BIBLE A and B campaigns, *J. Geophys. Res*, *107*, doi:10.1029/2001JD000800, in press, 2002.

Koike, M., et al., Impact of aircraft emissions on reactive nitrogen over the North Atlantic Flight Corridor region, *J. Geophys. Res.*, *105*, 3665–3677, 2000.

Koike, M., et al., Reactive nitrogen over the tropical western Pacific: Influence from lightning and biomass burning during BIBLE A, *J. Geophys. Res*, *107*, doi:10.1029/2001JD000823, in press, 2002.

Komala, N., S. Saraspriya, K. Kita, and T. Ogawa, Tropospheric ozone behaviour observed in Indonesia, *Atmos. Environ.*, *30*, 1851–1856, 1996.

Kondo, Y., S. Kawakami, M. Koike, D. W. Fahey, H. Nakajima, Y. Zhao, N. Toriyama, M. Kanada, G. W. Sachse, and G. W. Gregory, Performance of an aircraft instrument for the measurement of NOy, *J. Geophys. Res.*, *102*, 28,663–28,671, 1997.

Kondo, Y., et al., Effects of biomass burning, lightning, and convection on O_3, CO, and NO_y over the tropical Pacific and Australia in August–October 998 and 999, *J. Geophys. Res*, *107*, doi:10.1029/2001JD000820, in press, 2002.

Kotamarthi, V. R., et al., Evidence of heterogeneous chemistry on sulfate aerosols in stratospherically influenced air masses sampled during PEM-West B, *J. Geophys. Res.*, *102*, 28,425–28,436, 1997.

Matsueda, H., and H. Y. Inoue, Aircraft measurements of trace gases between Japan and Singapore in October of 1993, 1996, and 1997, *Geophys. Res. Lett.*, *26*, 2413–2416, 1999.

Matsuzono, T., T. Sano, and T. Ogawa, Development of the trajectory analysis model (EORC/TAM), *EORC Bull. Tech. Rep. 1*, edited by T. Igarashi, pp. 55–68, Natl. Space Dev. Agency of Jpn., Tokyo, 1998.

Nishi, N., Meteorological fields which affect the transport and chemical processes during the Biomass Burning and Lightning Experiment phase-A and B (BIBLE-A, B), in *EORC Bull. Tech. Rep. 7*, edited by T. Igarashi, pp. 36–52, 2001.

Novelli, P. C., J. W. Elkins, and L. P. Steele, The development and evaluation of a gravimetric reference scale for measurements of atmospheric carbon monoxide, *J. Geophys. Res.*, *96*, 13,109–13,121, 1991.

Novelli, P. C., K. A. Masarie, and P. M. Lang, Distribution and recent changes of carbon monoxide in the lower troposphere, *J. Geophys. Res.*, *103*, 19,015–19,033, 1998.

Pickering, K. E., A. M. Thompson, J. R. Scala, W.-K. Tao, J. Simpson, and M. Garstang, Photochemical ozone production in tropical ozone squall line convection during NASA Global Tropospheric Experiment/Amazon Boundary Layer Experiment 2A, *J. Geophys. Res.*, *96*, 3099–3144, 1991.

Pickering, K. E., A. M. Thompson, W.-K. Tao, and T. L. Kucsera, Upper tropospheric ozone production following mesoscale convection during STEP/EMEX, *J. Geophys. Res.*, *98*, 8737–8749, 1993.

Pickering, K. E., et al., Convective transport of biomass burning emissions over Brazil during TRACE A, *J. Geophys. Res.*, *101*, 23,993–24,012, 1996.

Proffitt, M. H., and R. J. McLaughlin, Fast-response dual-beam UV-absorption ozone photometer suitable for use on stratospheric balloons, *Rev. Sci. Inst.*, *54*, 1719–1728, 1983.

Robbins, R. C., K. M. Borg, and E. Robinson, Carbon monoxide in the atmosphere, *J. Air Pollut. Control Assoc.*, *18*, 106–110, 1968.

Sawa, Y., H. Matsueda, Y. Tsutumi, J. Jensen, H. Y. Inoue, and Y. Makino, CO and H_2 measurements over Kalimantan in Indonesia and northern Australia in October, 1997, *Geophys. Res. Lett.*, *26*, 1389–1392, 1999.

Schultz, M. G., et al., On the origin of tropospheric ozone and NOx over the tropical south Pacific, *J. Geophys. Res.*, *104*, 5829–5843, 1999.

Seiler, W., The cycle of atmospheric CO, *Tellus, Ser. B*, *26*, 118–135, 1974.

Shetter, R. E., and M. Müller, Photolysis frequency measurements using actinic flux spectroradiometry during the PEM-Tropics mission: Instrumentation description and some results, *J. Geophys. Res.*, *104*, 5647–5661, 1999.

Shirai, T., et al., Emission estimates of selected volatile organic compounds from tropical savanna burning in northern Australia, *J. Geophys. Res.*, *107*, doi:10.1029/2001JD000841, in press, 2002.

Thompson, A. M., and R. D. Hudson, Tropical tropospheric ozone (TTO) map from Nimbus 7 and Earth-Probe TOMS by the Modified-Residual method: Evaluation with sondes, ENSO signals and trends from Atlantic regional time series, *J. Geophys. Res.*, *104*, 26,941–26,975, 1999.

Thompson, A. M., J. C. Witte, R. D. Hudson, H. Guo, J. R. Herman, and M. Fujiwara, Tropical tropospheric ozone and biomass burning, *Science*, *291*, 2128–2132, 2001.

Tsutsumi, Y., Y. Sawa, Y. Makino, J. B. Jensen, J. L. Gras, B. F. Ryan, S. Diharto, and H. Harjanto, Aircraft measurements of ozone, NOx, CO, and aerosol concentrations in biomass burning smoke over Indonesia and

Australia in October 1997: Depleted ozone layer at low altitude over Indonesia, *Geophys. Res. Lett.*, *26*, 595–598, 1999.

Volz-Thomas, A., A. Lerner, H.-W. Pätz, M. Schultz, D. S. McKenna, R. Schmitt, S. Madronich, and E. P. Röth, Airborne measurements of the photolysis frequency of NO_2, *J. Geophys. Res.*, *101*, 18,613–18,627, 1996.

Wang, Y., W.-K. Tao, K. E. Pickering, A. M. Thompson, J. S. Kain, R. F. Adler, J. Simpson, P. R. Keehn, and G. S. Lai, Mesoscale model simulations of TRACE A and preliminary regional experiment for storm-scale operational and research meteorology convective systems and associated tracer transport, *J. Geophys. Res.*, *101*, 24,013–24,027, 1996.

Ziemke, J. R., and S. Chandra, Seasonal and interannual variabilities in tropical tropospheric ozone, *J. Geophys. Res.*, *104*, 21,425–21,442, 1999.

D. R. Blake, Department of Chemistry, University of California, Irvine, CA 92697-2025, USA. (dblake@orion.oac.uci.edu)

Y. Higashi, Y. Kondo, and Y. Miyazaki, Research Center for Advanced Science and Technology, University of Tokyo, 4-6-1 Komaba, Meguro-ku, Tokyo 153-8904, Japan. (yoko@aos.eps.s.u-tokyo.ac.jp; yuzom@aos.eps.s.u-tokyo.ac.jp)

W. Hu and M. Ko, Atmospheric and Environmental Research, Inc., 131 Hartwell Avenue, Lexington, MA 02421-3126, USA. (whu@aer.com; mko@aer.com)

S. Kawakami, T. Ogawa, and T. Sano, Earth Observation Research Center, National Space Development Agency of Japan, 1-8-10 Harumi, Chuou-ku, Tokyo 106-0032, Japan. (kawakami@eorc.nasda.go.jp; t_ogawa@eorc.nasda.go.jp; sano@eorc.nasda.go.jp)

K. Kita, Department of Environmental Sciences, Faculty of Science, Ibaraki University, 2-1-1 Bunkyo, Mito, Ibaraki 310-8512, Japan. (kita@env.sci.ibaraki.ac.jp)

M. Koike, Department of Earth and Planetary Science, Graduate School of Science, University of Tokyo, 7-3-1 Hongo, Bunkyo-ku, Tokyo 113-0033, Japan. (koike@eps.s.u-tokyo.ac.jp)

T. Machida, National Institute of Environmental Studies, 16-2 Onogawa, Tsukuba, Ibaraki, 305-8506, Japan. (tmachida@nies.go.jp)

N. Nishi, Department of Earth and Planetary Science, Graduate School of Science, Kyoto University, Kitashirakawa-Oiwakecho, Sakyo-ku, Kyoto 606-8502, Japan. (nishi@kugi.kyoto-u.ac.jp)

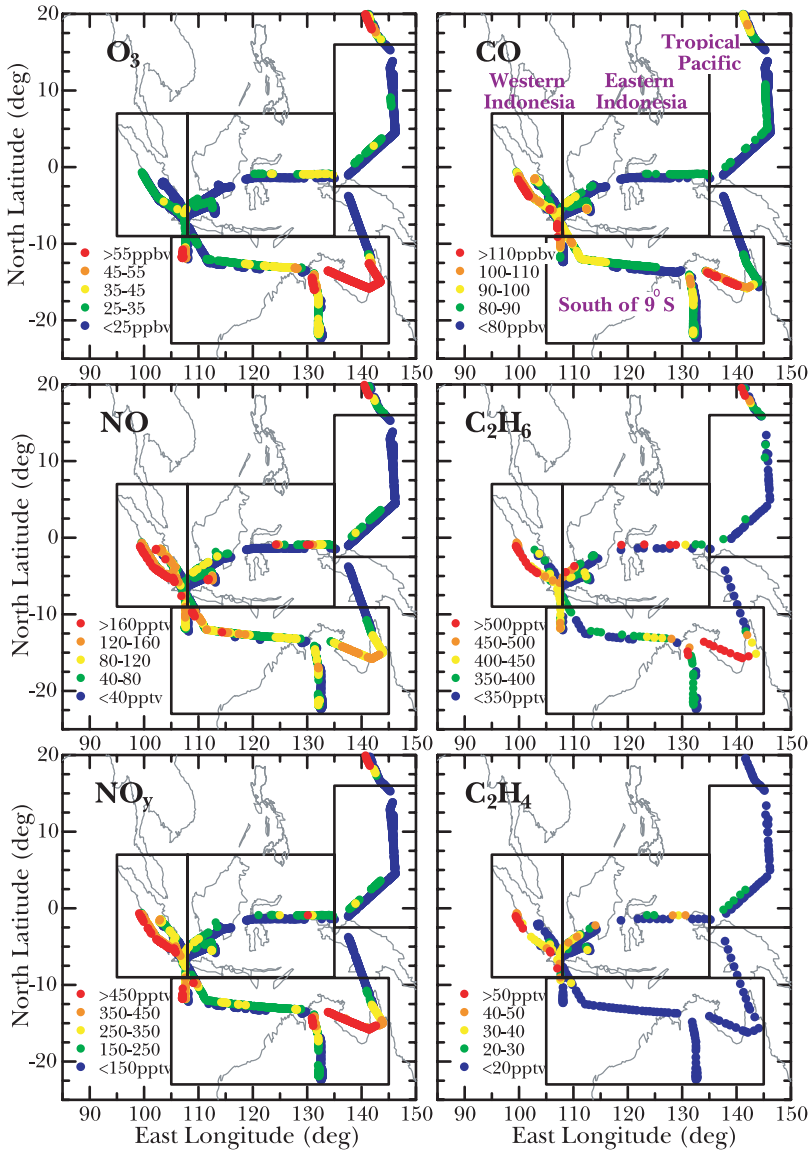

Figure 1. Distribution of ozone, NO, NO_y, CO, C_2H_6, and C_2H_4 in the upper troposphere (8–13.5 km) observed during BIBLE-A.

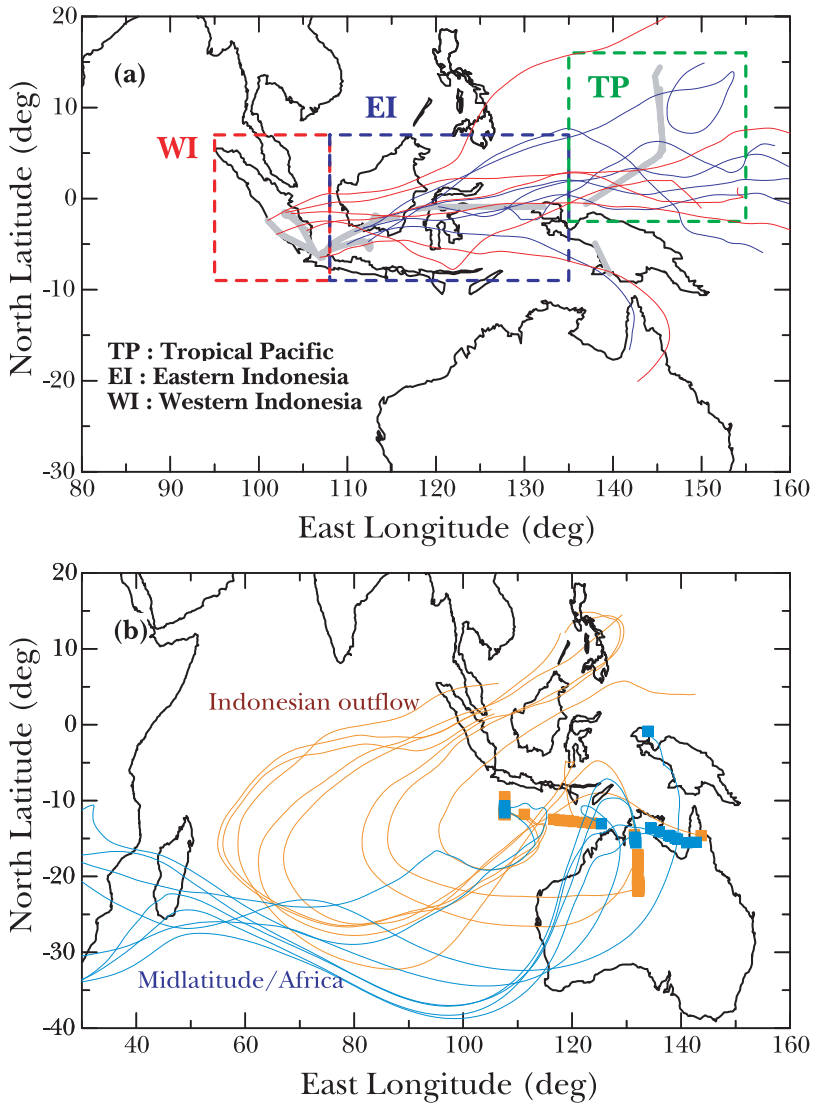

Figure 4. (a) Aircraft flight tracks (gray curves) above 8 km over the tropical Pacific Ocean (shown by box 'TP'), eastern Indonesia (shown by box 'EI'), and western Indonesia (shown by box 'WI') during BIBLE-A. Examples of backward trajectories from the flight tracks over eastern and western Indonesia are shown by blue and red curves, respectively. (b) Examples of backward trajectories (thin curves) from the observation points (squares) for the Indonesian outflow air (orange) and the midlatitude/African air (light blue).

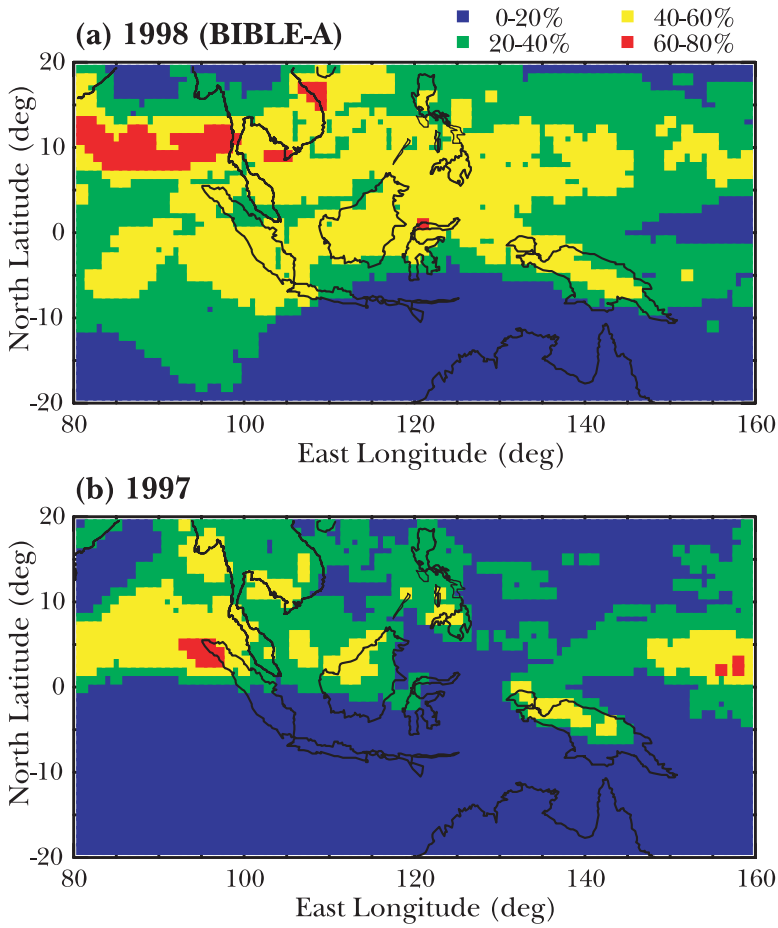

Figure 5. Occurrence distribution of high (>8 km), optically thick clouds in the Indonesian region between 24 September and 10 October in (a) 1998 and (b) 1997.